Chapter 12

Grasping and Manipulation

Most of the book so far has been concerned with kinematics, dynamics, motion planning, and control of the robot itself. Only in Chapter 11, on the topics of force control and impedance control, did the robot finally begin interacting with an environment other than free space. Now the robot really becomes valuable – when it can perform useful work on objects in the environment.

In this chapter our focus moves outward from the robot itself to the interaction between the robot and its environment. The desired behavior of the robot hand or end-effector, whether motion control, force control, hybrid motion–force control, or impedance control, is assumed to be achieved perfectly using the methods discussed so far. Our focus now is on the contact interface between the robot and objects as well as on contacts among objects and between objects and constraints in the environment. In short, our focus is on *manipulation* rather than the *manipulator*. Examples of manipulation include grasping, pushing, rolling, throwing, catching, tapping, etc. To limit our scope, we will assume that the manipulator, objects, and obstacles in the environment are rigid.

To simulate, plan, and control robotic manipulation tasks, we need an understanding of (at least) three elements: contact kinematics; forces applied through contacts; and the dynamics of rigid bodies. In contact kinematics we study how rigid bodies can move relative to each other without penetration and classify these feasible motions according to whether the contacts are rolling, sliding, or separating. Contact force models address the normal and frictional forces that can be transmitted through rolling and sliding contacts. Finally, the actual motions of the bodies are those that simultaneously satisfy the kinematic constraints, contact force model, and rigid-body dynamics.

This chapter introduces contact kinematics (Section 12.1) and contact force

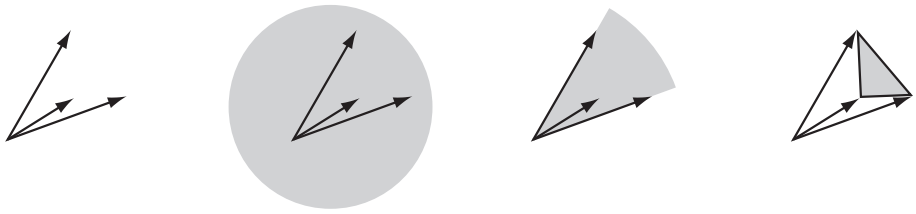

Figure 12.1: (a) Three vectors in $\mathbb{R}^2$, drawn as arrows from the origin. (b) The linear span of the vectors is the entire plane. (c) The positive linear span is the cone shaded gray. (d) The convex span is the polygon and its interior.

modeling (Section 12.2) and applies these models to problems in robot grasping and other types of manipulation.

The following definitions from linear algebra will be useful in this chapter.

Definition 12.1. Given a set of j vectors $\mathcal{A} = a_1, \ldots, a_j \in \mathbb{R}^n$, we define the **linear span**, or the set of linear combinations, of the vectors to be

$$\text{span}(\mathcal{A}) = \left\{ \sum_{i=1}^{j} k_i a_i \;\middle|\; k_i \in \mathbb{R} \right\},$$

the **nonnegative linear combinations**, sometimes called the **positive** or **conical span**, to be

$$\text{pos}(\mathcal{A}) = \left\{ \sum_{i=1}^{j} k_i a_i \;\middle|\; k_i \geq 0 \right\},$$

and the **convex span** to be

$$\text{conv}(\mathcal{A}) = \left\{ \sum_{i=1}^{j} k_i a_i \;\middle|\; k_i \geq 0 \text{ and } \sum_i k_i = 1 \right\}.$$

Clearly $\text{conv}(\mathcal{A}) \subseteq \text{pos}(\mathcal{A}) \subseteq \text{span}(\mathcal{A})$ (see Figure 12.1). The following facts from linear algebra will also be useful.

1. The space $\mathbb{R}^n$ can be linearly spanned by n vectors, but no fewer.
2. The space $\mathbb{R}^n$ can be positively spanned by $n+1$ vectors, but no fewer.

The first fact is implicit in our use of n coordinates to represent n-dimensional Euclidean space. Fact 2 follows from the fact that for any choice of n vectors $\mathcal{A} = \{a_1, \ldots, a_n\}$ there exists a vector $c \in \mathbb{R}^n$ such that $a_i^{\mathrm{T}} c \leq 0$ for all i. In other words, no nonnegative combination of vectors in $\mathcal{A}$ can create a vector in the direction c. However, if we choose $a_1, \ldots, a_n$ to be orthogonal coordinate bases of $\mathbb{R}^n$ and then choose $a_{n+1} = -\sum_{i=1}^{n} a_i$, we see that this set of $n+1$ vectors positively spans $\mathbb{R}^n$.

12.1 Contact Kinematics

Contact kinematics is the study of how two or more rigid bodies can move relative to each other while respecting the impenetrability constraint. It also classifies motion at a contact as either rolling or sliding. Let's start by looking at a single contact between two rigid bodies.

12.1.1 First-Order Analysis of a Single Contact

Consider two rigid bodies whose configurations are given by the local coordinate column vectors q_1 and q_2, respectively. Writing the composite configuration as $q = (q_1, q_2)$, we define a distance function $d(q)$ between the bodies that is positive when they are separated, zero when they are touching, and negative when they are in penetration. When $d(q) > 0$, there are no constraints on the motions of the bodies; each is free to move with six degrees of freedom. When the bodies are in contact ($d(q) = 0$), we look at the time derivatives $\dot{d}$, $\ddot{d}$, etc., to determine whether the bodies stay in contact or break apart as they follow a particular trajectory $q(t)$. This can be determined by the following table of possibilities:

d	$\dot{d}$	$\ddot{d}$	$\cdots$	
> 0				no contact
< 0				infeasible (penetration)
$= 0$	> 0			in contact, but breaking free
$= 0$	< 0			infeasible (penetration)
$= 0$	$= 0$	> 0		in contact, but breaking free
$= 0$	$= 0$	< 0		infeasible (penetration)
etc.				

The contact is maintained only if all time derivatives are zero.

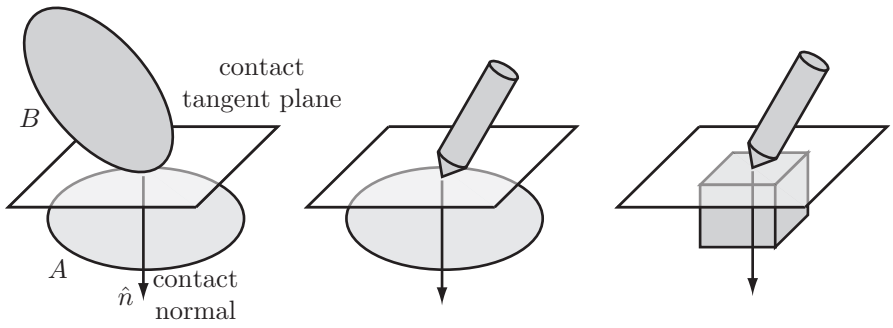

Figure 12.2: (Left) The bodies A and B in single-point contact define a contact tangent plane and a contact normal vector $\hat{n}$ perpendicular to the tangent plane. By default, the positive direction of the normal is chosen into body A. Since contact curvature is not addressed in this chapter, the contact places the same restrictions on the motions of the rigid bodies in the middle and right panels.

Now let's assume that the two bodies are initially in contact ($d = 0$) at a single point. The first two time derivatives of d are written

$$\dot{d} = \frac{\partial d}{\partial q}\dot{q}, \tag{12.1}$$

$$\ddot{d} = \dot{q}^{\mathrm{T}}\frac{\partial^2 d}{\partial q^2}\dot{q} + \frac{\partial d}{\partial q}\ddot{q}. \tag{12.2}$$

The terms $\partial d/\partial q$ and $\partial^2 d/\partial q^2$ carry information about the local contact geometry. The gradient vector $\partial d/\partial q$ corresponds to the separation direction in q space associated with the **contact normal** (Figure 12.2). The matrix $\partial^2 d/\partial q^2$ encodes information about the relative curvature of the bodies at the contact point.

In this chapter we assume that only contact-normal information $\partial d/\partial q$ is available at contacts; other information about the local contact geometry, including the contact curvature $\partial^2 d/\partial q^2$ and higher derivatives, is unknown. With this assumption, we truncate our analysis at Equation (12.1) and assume that the bodies remain in contact if $\dot{d} = 0$. Since we are dealing only with the first-order contact derivative $\partial d/\partial q$, we refer to our analysis as a *first-order* analysis. In such a first-order analysis, the contacts in Figure 12.2 are treated identically since they have the same contact normal.

As indicated in the table above, a *second-order* analysis incorporating the contact curvature $\partial^2 d/\partial q^2$ may indicate that the contact is actually breaking or penetrating even when $d = \dot{d} = 0$. We will see examples of this, but a detailed

analysis of second-order contact conditions is beyond the scope of this chapter.

12.1.2 Contact Types: Rolling, Sliding, and Breaking Free

Given two bodies in single-point contact, they undergo a **roll–slide motion** if the contact is maintained. The constraint that contact is maintained is a holonomic constraint, $d(q) = 0$. A necessary condition for maintaining contact is $\dot{d} = 0$.

Let's write the velocity constraint $\dot{d} = 0$ in a form, based on the contact normal, that does not require an explicit distance function (Figure 12.2). Let $\hat{n} \in \mathbb{R}^3$ be a unit vector aligned with the contact normal, expressed in a world frame. Let $p_A \in \mathbb{R}^3$ be the representation of the contact point on body A in the world frame, and let $p_B \in \mathbb{R}^3$ be the representation of the contact point on body B. Although the contact-point vectors p_A and p_B are identical initially, the velocities $\dot{p}_A$ and $\dot{p}_B$ may be different. Thus the condition $\dot{d} = 0$ can be written

$$\hat{n}^{\mathrm{T}}(\dot{p}_A - \dot{p}_B) = 0. \tag{12.3}$$

Since the direction of the contact normal is defined as being into body A, the impenetrability constraint $\dot{d} \geq 0$ is written as

$$\hat{n}^{\mathrm{T}}(\dot{p}_A - \dot{p}_B) \geq 0. \tag{12.4}$$

Let us rewrite the constraint (12.4) in terms of the twists $\mathcal{V}_A = (\omega_A, v_A)$ and $\mathcal{V}_B = (\omega_B, v_B)$ of bodies A and B in a space frame.[1] Note that

$$\begin{aligned} \dot{p}_A &= v_A + \omega_A \times p_A = v_A + [\omega_A]p_A, \\ \dot{p}_B &= v_B + \omega_B \times p_B = v_B + [\omega_B]p_B. \end{aligned}$$

We can also define the wrench $\mathcal{F} = (m, f)$ corresponding to a unit force applied along the contact normal:

$$\mathcal{F} = (p_A \times \hat{n}, \hat{n}) = ([p_A]\hat{n}, \hat{n}).$$

It is not necessary to appeal to forces in a purely kinematic analysis of rigid bodies, but we will find it convenient to adopt this notation now in anticipation of the discussion of contact forces in Section 12.2.

With these expressions, the inequality constraint (12.4) can be written

$$\textbf{(impenetrability constraint)} \qquad \mathcal{F}^{\mathrm{T}}(\mathcal{V}_A - \mathcal{V}_B) \geq 0 \tag{12.5}$$

[1] All twists and wrenches are expressed in a space frame in this chapter.

(see Exercise 12.1). If

$$\textbf{(active constraint)} \qquad \mathcal{F}^{\mathrm{T}}(\mathcal{V}_A - \mathcal{V}_B) = 0 \tag{12.6}$$

then, to first order, the constraint is active and the bodies remain in contact.

In the case where B is a stationary fixture, the impenetrability constraint (12.5) simplifies to

$$\mathcal{F}^{\mathrm{T}}\mathcal{V}_A \geq 0. \tag{12.7}$$

If $\mathcal{F}^{\mathrm{T}}\mathcal{V}_A > 0$, $\mathcal{F}$ and $\mathcal{V}_A$ are said to be **repelling**. If $\mathcal{F}^{\mathrm{T}}\mathcal{V}_A = 0$, $\mathcal{F}$ and $\mathcal{V}_A$ are said to be **reciprocal** and the constraint is active.

Twists $\mathcal{V}_A$ and $\mathcal{V}_B$ satisfying (12.6) are called **first-order roll–slide motions** – the contact may be either sliding or rolling. **Roll–slide contacts** may be further separated into **rolling contacts** and **sliding contacts**. The contact is rolling if the bodies have no motion relative to each other at the contact:

$$\textbf{(rolling constraint)} \qquad \dot{p}_A = v_A + [\omega_A]p_A = v_B + [\omega_B]p_B = \dot{p}_B. \tag{12.8}$$

Note that "rolling" contacts include those where the two bodies remain stationary relative to each other, i.e., no relative rotation. Thus "sticking" is another term for these contacts.

If the twists satisfy Equation (12.6) but not the rolling equations of (12.8) then they are sliding.

We assign to a rolling contact the **contact label** `R`, to a sliding contact the label `S`, and to a contact that is breaking free (the impenetrability constraint (12.5) is satisfied but not the active constraint (12.6)) the label `B`.

The distinction between rolling and sliding contacts becomes especially important when we consider friction forces in Section 12.2.

Example 12.2. Consider the contact shown in Figure 12.3. Bodies A and B are in contact at $p_A = p_B = [1\ 2\ 0]^{\mathrm{T}}$ with contact normal direction $\hat{n} = [0\ 1\ 0]^{\mathrm{T}}$. The impenetrability constraint (12.5) is

$$\mathcal{F}^{\mathrm{T}}(\mathcal{V}_A - \mathcal{V}_B) \geq 0,$$

which becomes

$$[([p_A]\hat{n})^{\mathrm{T}} \ \ \hat{n}^{\mathrm{T}}] \begin{bmatrix} \omega_A - \omega_B \\ v_A - v_B \end{bmatrix} \geq 0.$$

Substituting values, we obtain

$$[0\ 0\ 1\ 0\ 1\ 0][\omega_{Ax} - \omega_{Bx}\ \omega_{Ay} - \omega_{By}\ \omega_{Az} - \omega_{Bz}\ v_{Ax} - v_{Bx}\ v_{Ay} - v_{By}\ v_{Az} - v_{Bz}]^{\mathrm{T}} \geq 0$$

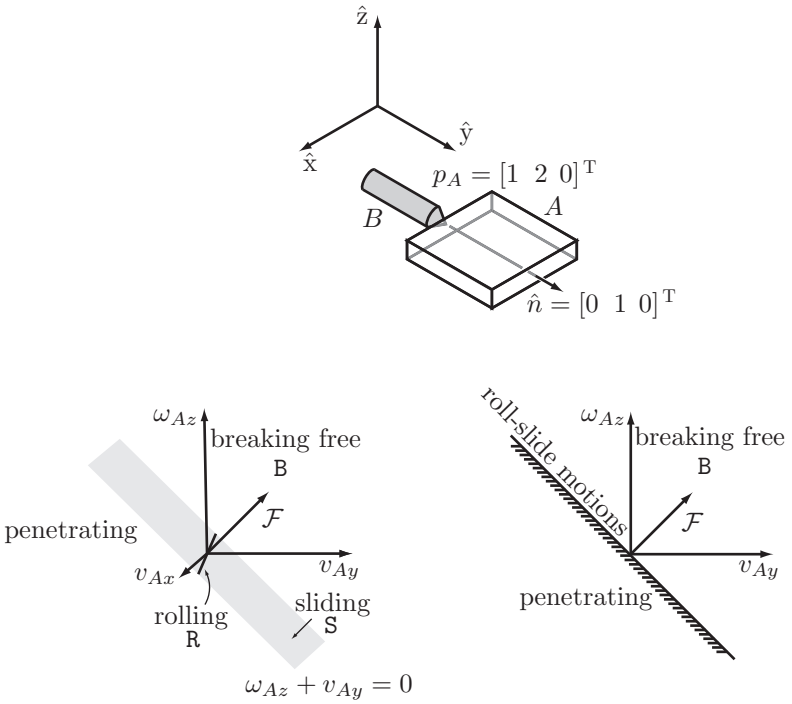

Figure 12.3: Example 12.2. (Top) Body B makes contact with A at $p_A = p_B = [1\ 2\ 0]^{\mathrm{T}}$ with normal $\hat{n} = [0\ 1\ 0]^{\mathrm{T}}$. (Bottom left) The twists $\mathcal{V}_A$ and their corresponding contact labels for B stationary and A confined to a plane. The contact normal wrench $\mathcal{F}$ is $[m_x\ m_y\ m_z\ f_x\ f_y\ f_z]^{\mathrm{T}} = [0\ 0\ 1\ 0\ 1\ 0]^{\mathrm{T}}$. (Bottom right) Looking down the $-v_{Ax}$-axis.

or

$$\omega_{Az} - \omega_{Bz} + v_{Ay} - v_{By} \geq 0;$$

and therefore roll–slide twists satisfy

$$\omega_{Az} - \omega_{Bz} + v_{Ay} - v_{By} = 0. \tag{12.9}$$

Equation (12.9) defines an 11-dimensional hyperplane in the 12-dimensional space of twists $(\mathcal{V}_A, \mathcal{V}_B)$.

The rolling constraint (12.8) is equivalent to

$$\begin{aligned} v_{Ax} - \omega_{Az} p_{Ay} + \omega_{Ay} p_{Az} &= v_{Bx} - \omega_{Bz} p_{By} + \omega_{By} p_{Bz}, \\ v_{Ay} + \omega_{Az} p_{Ax} - \omega_{Ax} p_{Az} &= v_{By} + \omega_{Bz} p_{Bx} - \omega_{Bx} p_{Bz}, \\ v_{Az} + \omega_{Ax} p_{Ay} - \omega_{Ay} p_{Ax} &= v_{Bz} + \omega_{Bx} p_{By} - \omega_{By} p_{Bx}; \end{aligned}$$

substituting values for p_A and p_B, we get

$$v_{Ax} - 2\omega_{Az} = v_{Bx} - 2\omega_{Bz}, \tag{12.10}$$

$$v_{Ay} + \omega_{Az} = v_{By} + \omega_{Bz}, \tag{12.11}$$

$$v_{Az} + 2\omega_{Ax} - \omega_{Ay} = v_{Bz} + 2\omega_{Bx} - \omega_{By}. \tag{12.12}$$

The constraint equations (12.10)–(12.12) define a nine-dimensional hyperplane subspace of the 11-dimensional hyperplane of roll–slide twists.

To visualize the constraints in a low-dimensional space, let's assume that B is stationary ($\mathcal{V}_B = 0$) and A is confined to the $z = 0$ plane, i.e., $\mathcal{V}_A = [\omega_{Ax}\ \omega_{Ay}\ \omega_{Az}\ v_{Ax}\ v_{Ay}\ v_{Az}]^{\mathrm{T}} = [0\ 0\ \omega_{Az}\ v_{Ax}\ v_{Ay}\ 0]^{\mathrm{T}}$. The wrench $\mathcal{F}$ is written $[m_z\ f_x\ f_y]^{\mathrm{T}} = [1\ 0\ 1]^{\mathrm{T}}$. The roll–slide constraint (12.9) reduces to

$$v_{Ay} + \omega_{Az} = 0,$$

while the rolling constraints simplify to

$$\begin{aligned} v_{Ax} - 2\omega_{Az} &= 0, \\ v_{Ay} + \omega_{Az} &= 0. \end{aligned}$$

The single roll–slide constraint yields a plane in $(\omega_{Az}, v_{Ax}, v_{Ay})$ space, and the two rolling constraints yield a line in that plane. Because $\mathcal{V}_B = 0$, the constraint surfaces pass through the origin $\mathcal{V}_A = 0$. If $\mathcal{V}_B \neq 0$, this is no longer the case in general.

Figure 12.3 shows graphically that nonpenetrating twists $\mathcal{V}_A$ must have a nonnegative dot product with the constraint wrench $\mathcal{F}$ when $\mathcal{V}_B = 0$.

12.1.3 Multiple Contacts

Now suppose that a body A is subject to n contacts with m other bodies, where $n \geq m$. The contacts are numbered $i = 1, \ldots, n$, and the other bodies are numbered $j = 1, \ldots, m$. Let $j(i) \in \{1, \ldots, m\}$ denote the number of the other body participating in contact i. Each contact i constrains $\mathcal{V}_A$ to a half-space of its six-dimensional twist space that is bounded by a five-dimensional hyperplane of the form $\mathcal{F}^{\mathrm{T}}\mathcal{V}_A = \mathcal{F}^{\mathrm{T}}\mathcal{V}_{j(i)}$. Taking the union of the set of constraints from

all the contacts, we get a **polyhedral convex set** (**polytope**[2] for short) V of feasible twists in the $\mathcal{V}_A$ space, written as

$$V = \{\mathcal{V}_A \mid \mathcal{F}_i^{\mathrm{T}}(\mathcal{V}_A - \mathcal{V}_{j(i)}) \geq 0 \text{ for all } i\},$$

where $\mathcal{F}_i$ corresponds to the ith contact normal (pointing into the body A) and $\mathcal{V}_{j(i)}$ is the twist of the other body at contact i. The constraint at contact i is redundant if the half-space constraint contributed by contact i does not change the feasible twist polytope V. In general, the feasible twist polytope for a body can consist of a six-dimensional interior (where no contact constraint is active), five-dimensional faces where one constraint is active, four-dimensional faces where two constraints are active, and so on, down to one-dimensional edges and zero-dimensional points. A twist $\mathcal{V}_A$ on a k-dimensional facet of the polytope indicates that $6-k$ independent (non-redundant) contact constraints are active.

If all the bodies providing constraints are stationary, i.e., $\mathcal{V}_j = 0$ for all j, then each constraint hyperplane defined by (12.5) passes through the origin of $\mathcal{V}_A$ space. We call such a constraint **homogeneous**. The feasible twist set becomes a cone rooted at the origin, called a (homogeneous) **polyhedral convex cone**. Let $\mathcal{F}_i$ be the constraint wrench of stationary contact i. Then the feasible twist cone V is

$$V = \{\mathcal{V}_A \mid \mathcal{F}_i^{\mathrm{T}}\mathcal{V}_A \geq 0 \text{ for all } i\}.$$

If the $\mathcal{F}_i$ positively span the six-dimensional wrench space or, equivalently, the convex span of the $\mathcal{F}_i$ contains the origin in the interior then the feasible twist polytope V reduces to a point at the origin, the stationary contacts completely constrain the motion of the body, and we have **form closure**, discussed in more detail in Section 12.1.7.

As mentioned in Section 12.1.2, each point contact i can be given a label corresponding to the type of contact: `B` if the contact is breaking, `R` if the contact is rolling, and `S` if the contact is sliding, i.e., (12.6) is satisfied but (12.8) is not. The **contact mode** for the entire system can be written as the concatenation of the contact labels at the contacts. Since we have three distinct contact labels, a system of bodies with n contacts can have a maximum of 3^n contact labels. Some of these contact modes may not be feasible, as their corresponding kinematic constraints may not be compatible.

[2] We use the term "polytope" to refer generally to a convex set bounded by hyperplanes in an arbitrary vector space. The set need not be finite; it could be a cone with infinite volume. It could also be a point, or the null set if the constraints are incompatible with the rigid-body assumption.

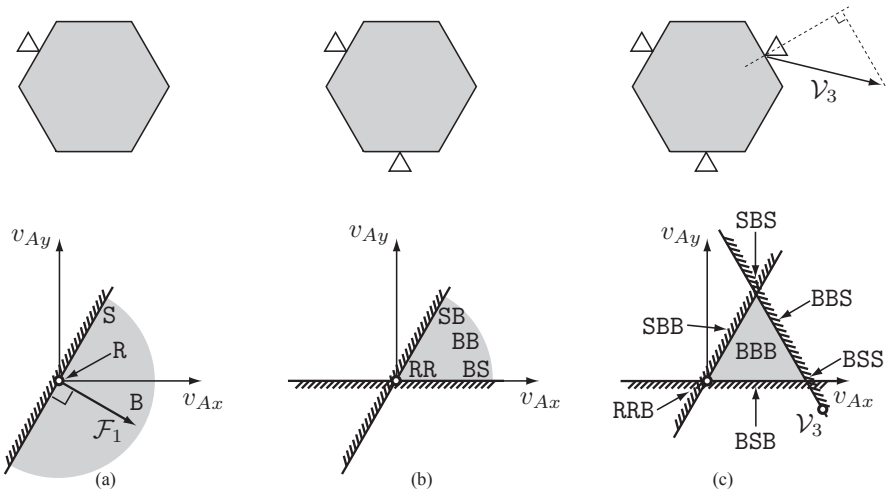

Figure 12.4: Motion-controlled fingers contacting a hexagon that is constrained to translate in a plane only (Example 12.3). (a) A single stationary finger provides a single half-space constraint on the hexagon's twist $\mathcal{V}_A$. The feasible-motion half-space is shaded gray. The two-dimensional set of twists corresponding to breaking contact `B`, the one-dimensional set corresponding to sliding contact `S`, and the zero-dimensional set corresponding to rolling (fixed) contact `R` are shown. (b) The union of constraints from two stationary fingers creates a cone of feasible twists. This cone corresponds to four possible contact modes: `RR`, `SB`, `BS`, and `BB`. The contact label for the finger at upper left is given first. (c) Three fingers, one of which is moving with a linear velocity $\mathcal{V}_3$, create a closed polygon of feasible twists. There are seven possible contact modes corresponding to the feasible twists: a two-dimensional set where all contacts are breaking, three one-dimensional sets where one contact constraint is active, and three zero-dimensional sets where two contact constraints are active. Note that rolling contact at the moving finger is not feasible, since translation of the hexagon to "follow" the moving finger, as indicated by the $\circ$ at the lower right of the lower figure, would violate one of the impenetrability constraints. If the third finger were stationary, the only feasible motion of the hexagon would be zero velocity, with contact mode `RRR`.

Example 12.3. Figure 12.4 shows triangular fingers contacting a hexagonal body A. To more easily visualize the contact constraints the hexagon is restricted to translational motion in a plane only, so that its twist can be written $\mathcal{V}_A = (0, 0, 0, v_{Ax}, v_{Ay}, 0)$. In Figure 12.4(a) the single stationary finger creates a contact wrench $\mathcal{F}_1$ that can be drawn in $\mathcal{V}_A$ space. All feasible twists have a nonnegative component in the direction of $\mathcal{F}_1$. Roll–slide twists satisfying $\mathcal{F}_1^{\mathrm{T}}\mathcal{V}_A = 0$ lie on the constraint line. Since no rotations are allowed, the only

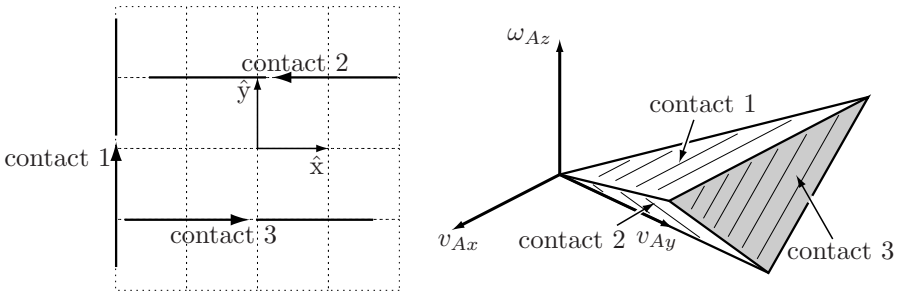

Figure 12.5: Example 12.4. (Left) Arrows representing the lines of force corresponding to the contact normals of three stationary contacts on a planar body. If we are concerned only with feasible motions, and do not distinguish between rolling and sliding, contacts anywhere along the lines, with the contact normals shown, are equivalent. (Right) The three constraint half-spaces define a polyhedral convex cone of feasible twists. In the figure the cone is truncated at the plane $v_{Ay} = 2$. The outer faces of the cone are indicated by hatching on a white background, and the inner faces by hatching on a gray background. Twists in the interior of the cone correspond to all contacts breaking, while twists on the faces of the cone correspond to one active constraint and twists on one of the three edges of the cone correspond to two active constraints.

twist yielding a rolling contact is $\mathcal{V}_A = 0$. In Figure 12.4(b) the union of the constraints due to two stationary fingers creates a (polyhedral convex) cone of feasible twists. Figure 12.4(c) shows three fingers in contact, one of which is moving with twist $\mathcal{V}_3$. Because the moving finger has nonzero velocity, its constraint half-space is displaced from the origin by $\mathcal{V}_3$. The result is a closed polygon of feasible twists.

Example 12.4. Figure 12.5 shows the contact normals of three stationary contacts with a planar body A, not shown. The body moves in a plane, so $v_{Az} = \omega_{Ax} = \omega_{Ay} = 0$. In this example we do not distinguish between rolling and sliding motions, so the locations of the contacts along the normals are irrelevant. The three contact wrenches, written (m_z, f_x, f_y), are $\mathcal{F}_1 = (0, 1, -2), \mathcal{F}_2 = (-1, 0, 1)$, and $\mathcal{F}_3 = (1, 0, 1)$, yield the motion constraints

$$\begin{aligned} v_{Ay} - 2\omega_{Az} &\geq 0, \\ -v_{Ax} + \omega_{Az} &\geq 0, \\ v_{Ax} + \omega_{Az} &\geq 0. \end{aligned}$$

These constraints describe a polyhedral convex cone of feasible twists rooted at the origin, as illustrated on the right in Figure 12.5.

12.1.4 Collections of Bodies

The discussion above can be generalized to find the feasible twists of multiple bodies in contact. If bodies i and j make contact at a point p, where $\hat{n}$ points into body i and $\mathcal{F} = ([p]\hat{n}, \hat{n})$ then their spatial twists $\mathcal{V}_i$ and $\mathcal{V}_j$ must satisfy the constraint

$$\mathcal{F}^{\mathrm{T}}(\mathcal{V}_i - \mathcal{V}_j) \geq 0 \tag{12.13}$$

to avoid penetration. This is a homogeneous half-space constraint in the composite $(\mathcal{V}_i, \mathcal{V}_j)$ twist space. In an assembly of m bodies, each pairwise contact contributes another constraint in the $6m$-dimensional composite twist space ($3m$-dimensional for planar bodies) and the result is a polyhedral convex cone of kinematically feasible twists rooted at the origin of the composite twist space. The contact mode for the entire assembly is the concatenation of the contact labels at each contact in the assembly.

If there are bodies whose motion is controlled, e.g., robot fingers, the constraints on the motion of the remaining bodies are no longer homogeneous. As a result, the convex polyhedral set of feasible twists of the uncontrolled bodies, in their composite twist space, is no longer a cone rooted at the origin.

12.1.5 Other Types of Contacts

We have been considering point contacts of the type shown in Figure 12.6(a), where at least one of the bodies in contact uniquely defines the contact normal. Figures 12.6(b)–(e) show other types of contact. The kinematic constraints provided by the convex–concave vertex, line, and plane contacts of Figures 12.6(b)–(d) are, to first order, identical to those provided by finite collections of single-point contacts. The degenerate case in Figure 12.6(e) is ignored, as there is no unique definition of a contact normal.

The impenetrability constraint (12.5) derives from the fact that arbitrarily large contact forces can be applied in the normal direction to prevent penetration. In Section 12.2, we will see that tangential forces due to friction may also be applied, and these forces may prevent slipping between two bodies in contact. Normal and tangential contact forces are subject to constraints: the normal force must be pushing into a body, not pulling, and the maximum friction force is proportional to the normal force.

If we wish to apply a kinematic analysis that can approximate the effects of friction without explicitly modeling forces, we can define three purely kinematic models of point contacts: a **frictionless point contact**, a **point contact with friction**, and a **soft contact**, also called a soft-finger contact. A frictionless point contact enforces only the roll–slide constraint (12.5). A point contact with

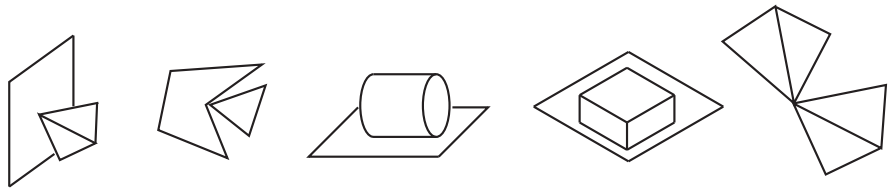

Figure 12.6: (a) Vertex–face contact. (b) The contact between a convex vertex and a concave vertex can be treated as multiple point contacts, one at each face adjacent to the concave vertex. These faces define the contact normals. (c) A line contact can be treated as two point contacts at either end of the line. (d) A plane contact can be treated as point contacts at the corners of the convex hull of the contact area. (e) Convex vertex–vertex contact. This case is degenerate and so is not considered.

friction also enforces the rolling constraints (12.8), implicitly modeling friction forces sufficient to prevent slip at the contact. A soft contact enforces the rolling constraints (12.8) as well as one more constraint: the two bodies in contact may not spin relative to each other about the contact normal axis. This models deformation and the resulting friction moment resisting any spin due to the nonzero contact area between the two bodies. For planar problems, a point contact with friction and a soft contact are identical.

12.1.6 Planar Graphical Methods

Planar problems allow the possibility of using graphical methods to visualize the feasible motions for a single body, since the space of twists is three dimensional. An example planar twist cone is shown in Figure 12.5. Such a figure would be very difficult to draw for a system with more than three degrees of freedom.

A convenient way to represent a planar twist, $\mathcal{V} = (\omega_z, v_x, v_y)$, in $\{s\}$ is as a **center of rotation** (CoR) at $(-v_y/\omega_z, v_x/\omega_z)$ plus the angular velocity ω_z. The CoR is the point in the (projective) plane that remains stationary under the motion, i.e., the point where the screw axis intersects the plane.[3] In the case where the speed of motion is immaterial, we may simply label the CoR with a '+', '−', or 0 sign representing the direction of rotation (Figure 12.7). The mapping from planar twists to CoRs is illustrated in Figure 12.8, which shows that the space of CoRs consists of a plane of '+' CoRs (counterclockwise), a plane of '−' CoRs (clockwise), and a circle of translation directions.

[3]Note that the case $\omega_z = 0$ must be treated with care, as it corresponds to a CoR at infinity.

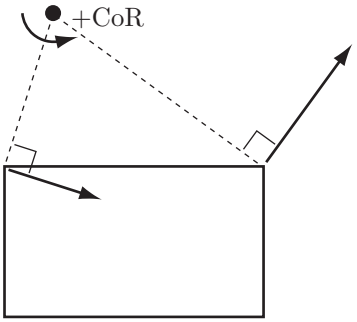

Figure 12.7: Given the velocity of two points on a planar body, the lines normal to the velocities intersect at the CoR. The CoR shown is labeled '+' corresponding to the (counterclockwise) positive angular velocity of the body.

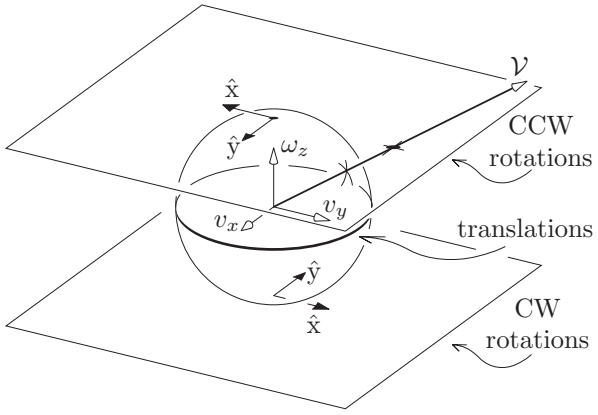

Figure 12.8: Mapping a planar twist $\mathcal{V}$ to a CoR. The ray containing the vector $\mathcal{V}$ intersects the plane of '+' CoRs at $\omega_z = 1$, or the plane of '−' CoRs at $\omega_z = -1$, or the circle of translation directions.

Given two different twists $\mathcal{V}_1$ and $\mathcal{V}_2$ and their corresponding CoRs, the set of linear combinations of these twists, $k_1\mathcal{V}_1 + k_2\mathcal{V}_2$ where $k_1, k_2 \in \mathbb{R}$, corresponds to the line of CoRs passing through $\text{CoR}(\mathcal{V}_1)$ and $\text{CoR}(\mathcal{V}_2)$. Since k_1 and k_2 can have either sign, it follows that if either ω_{1z} or ω_{2z} is nonzero then the CoRs on this line can have either sign. If $\omega_{1z} = \omega_{2z} = 0$ then the set of linear combinations corresponds to the set of all translation directions.

A more interesting case is when $k_1, k_2 \geq 0$. Given two twists $\mathcal{V}_1$ and $\mathcal{V}_2$, the

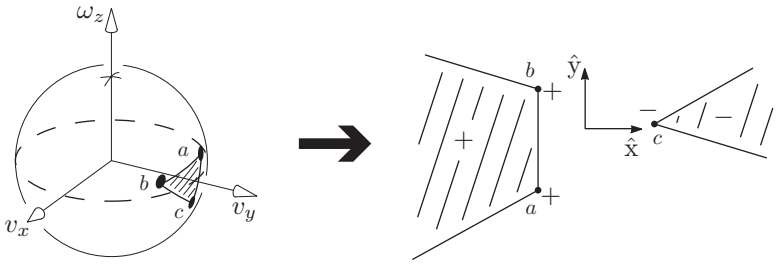

Figure 12.9: The intersection of a twist cone with the unit twist sphere, and the representation of the cone as a set of CoRs (the two hatched regions join at infinity to form a single set).

nonnegative linear combination of these two velocities is written

$$V = \text{pos}(\{\mathcal{V}_1, \mathcal{V}_2\}) = \{k_1\mathcal{V}_1 + k_2\mathcal{V}_2 \mid k_1, k_2 \geq 0\},$$

which is a planar twist cone rooted at the origin, with $\mathcal{V}_1$ and $\mathcal{V}_2$ defining the edges of the cone. If ω_{1z} and ω_{2z} have the same sign then the CoRs of their nonnegative linear combinations $\text{CoR}(\text{pos}(\{\mathcal{V}_1, \mathcal{V}_2\}))$ all have that sign and lie on the line segment between the two CoRs. If $\text{CoR}(\mathcal{V}_1)$ and $\text{CoR}(\mathcal{V}_2)$ are labeled '+' and '−' respectively, then $\text{CoR}(\text{pos}(\{\mathcal{V}_1, \mathcal{V}_2\}))$ consists of the line containing the two CoRs, minus the segment between the CoRs. This set consists of a ray of CoRs labeled '+' attached to $\text{CoR}(\mathcal{V}_1)$, a ray of CoRs labeled '−' attached to $\text{CoR}(\mathcal{V}_2)$, and a point at infinity labeled 0, corresponding to translation. This collection of elements should be considered as a single line segment (though one passing through infinity), just like the first case mentioned above. Figures 12.9 and 12.10 show examples of CoR regions corresponding to positive linear combinations of planar twists.

The CoR representation of planar twists is particularly useful for representing the feasible motions of one movable body in contact with stationary bodies. Since the constraints are stationary, as noted in Section 12.1.3, the feasible twists form a polyhedral convex cone rooted at the origin. Such a cone can be represented uniquely by a set of CoRs with '+', '−', and 0 labels. A general twist polytope, as would be generated by moving constraints, cannot be uniquely represented by a set of CoRs with such labels.

Given a contact between a stationary body and a movable body, we can plot the CoRs that do not violate the impenetrability constraint. Label all points on the contact normal '±', points to the left of the inward normal '+', and points to the right '−'. All points labeled '+' can serve as CoRs with positive angular velocity for the movable body, and all points labeled '−' can serve as CoRs with

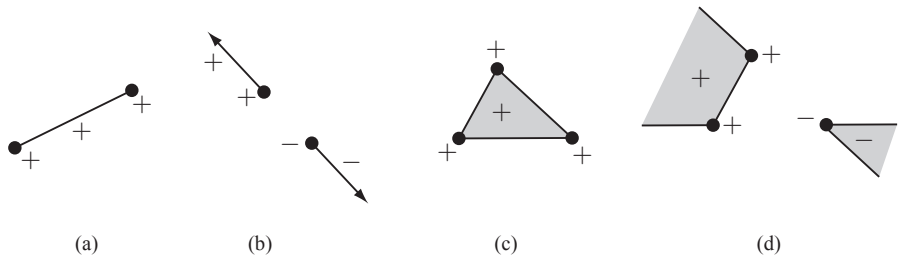

Figure 12.10: (a) Positive linear combination of two CoRs labeled '+'. (b) Positive linear combination of a '+' CoR and a '−' CoR. (c) Positive linear combination of three '+' CoRs. (d) Positive linear combination of two '+' CoRs and a '−' CoR.

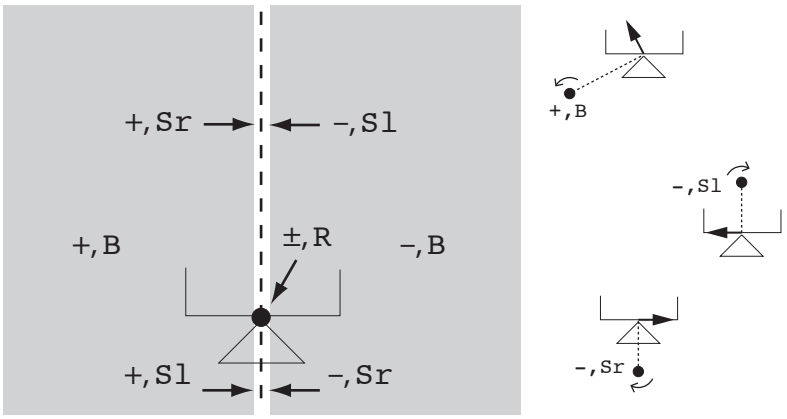

Figure 12.11: The stationary triangle makes contact with a movable body. The CoRs to the left of the contact normal are labeled '+', to the right are labeled '−', and on the normal are labeled '±'. Also given are the contact labels for the CoRs. For points on the contact normal, the sign assigned to the `Sl` and `Sr` CoRs switches at the contact point. Three CORs and their associated labels are illustrated.

negative angular velocity, without violating the first-order contact constraint. We can further assign contact labels to each CoR corresponding to the first-order conditions for breaking contact `B`, sliding contact `S`, or rolling contact `R`. For planar sliding, we subdivide the label `S` into two subclasses: `Sr`, where the moving body slips to the right relative to the fixed constraint, and `Sl`, where the moving body slips to the left. Figure 12.11 illustrates the labeling.

If there is more than one contact, we simply take the union of the constraints and contact labels from the individual contacts. This unioning of the constraints

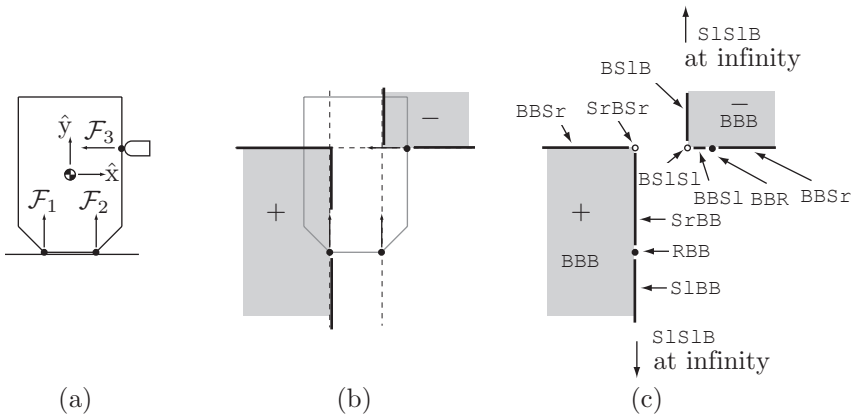

Figure 12.12: Example 12.5. (a) A body resting on a table with two contact constraints provided by the table and a single contact constraint provided by the stationary finger. (b) The feasible twists represented as CoRs, shown in gray. Note that the lines that extend off to the left and to the bottom "wrap around" at infinity and come back in from the right and the top, respectively, so this CoR region should be interpreted as a single connected convex region. (c) The contact modes assigned to each feasible motion. The zero velocity contact mode is `RRR`.

implies that the feasible CoR region is convex, as is the homogeneous polyhedral twist cone.

Example 12.5. Figure 12.12(a) shows a planar body standing on a table while being contacted by a stationary robot finger. The finger defines an inequality constraint on the body's motion and the table defines two more. The cone of twists that do not violate the impenetrability constraints is represented by the CoRs that are consistently labeled for each contact (Figure 12.12(b)). Each feasible CoR is labeled with a contact mode that concatenates the labels for the individual contacts (Figure 12.12(c)).

Now look more closely at the CoR indicated by (+, `SrBSr`) in Figure 12.12(c). Is this motion really possible? It should be apparent that it is, in fact, *not* possible: the body would immediately penetrate the stationary finger. Our incorrect conclusion that the motion was possible was due to the fact that our first-order analysis ignored the local contact curvature. A second-order analysis would show that this motion is indeed impossible. However, if the radius of curvature of the body at the contact were sufficiently small then the motion would be possible.

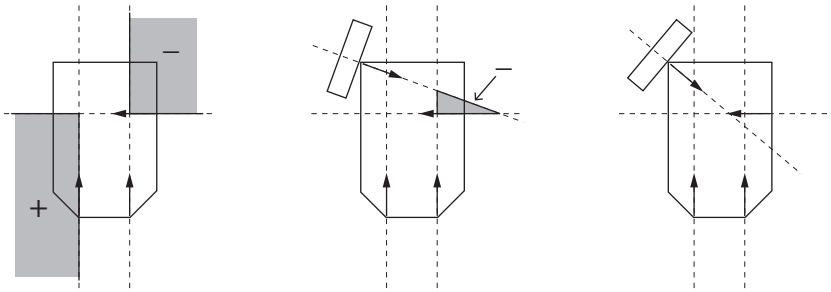

Figure 12.13: (Left) The body from Figure 12.12, with three stationary point contacts and the body's feasible twist cone represented as a convex CoR region. (Middle) A fourth contact reduces the size of the feasible twist cone. (Right) By changing the angle of the fourth contact normal, no twist is feasible; the body is in form closure.

Thus a first-order roll–slide motion might be classified as penetrating or breaking by a second-order analysis. Similarly, if our second-order analysis indicates a roll–slide motion, a third- or higher-order analysis may indicate penetration or breaking free. In any case, if an nth-order analysis indicates that the contact is breaking or penetrating, then no analysis of order greater than n will change the conclusion.

12.1.7 Form Closure

Form closure of a body is achieved if a set of stationary constraints prevents all motion of the body. If these constraints are provided by robot fingers, we call this a **form-closure grasp**. An example is shown in Figure 12.13.

12.1.7.1 Number of Contacts Needed for First-Order Form Closure

Each stationary contact i provides a half-space twist constraint of the form

$$\mathcal{F}_i^{\mathrm{T}}\mathcal{V} \geq 0.$$

Form closure holds if the only twist $\mathcal{V}$ satisfying the constraints is the zero twist. For j contacts, this condition is equivalent to

$$\mathrm{pos}(\{\mathcal{F}_1, \ldots, \mathcal{F}_j\}) = \mathbb{R}^6$$

for bodies in three dimensions. Therefore, by fact 2 from the beginning of the chapter, at least $6 + 1 = 7$ contacts are needed for the first-order form closure

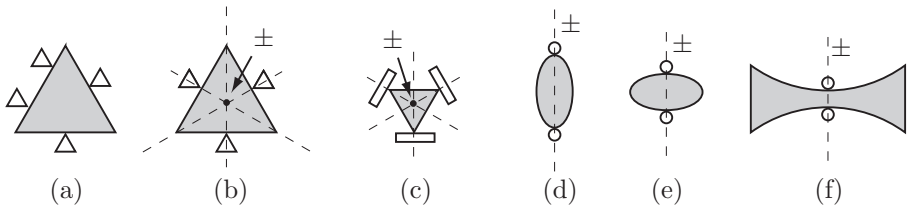

Figure 12.14: (a) Four fingers yielding planar form closure. The first-order analysis treats (b) and (c) identically, saying that the triangle can rotate about its center in each case. A second-order analysis shows this is not possible for (b). The grasps in (d), (e), and (f) are identical by a first-order analysis, which says that rotation about any center on the vertical line is possible. This is true for (d), while for (e), rotation if possible about only some of these centers. No motion is possible in (f).

of spatial bodies. For planar bodies, the condition is

$$\text{pos}(\{\mathcal{F}_1, \ldots, \mathcal{F}_j\}) = \mathbb{R}^3,$$

and $3 + 1 = 4$ contacts are needed for first-order form closure. These results are summarized in the following theorem.

Theorem 12.6. *For a planar body, at least four point contacts are needed for first-order form closure. For a spatial body, at least seven point contacts are needed.*

Now consider the problem of grasping a circular disk in the plane. It should be clear that kinematically preventing motion of the disk is impossible regardless of the number of contacts; it will always be able to spin about its center. Such objects are called **exceptional** – the positive span of the contact normal forces at all points on the object is not equal to $\mathbb{R}^n$, where $n = 3$ in the planar case and $n = 6$ in the spatial case. Examples of such objects in three dimensions include surfaces of revolution, such as spheres and ellipsoids.

Figure 12.14 shows examples of planar grasps. The graphical methods of Section 12.1.6 indicate that the four contacts in Figure 12.14(a) immobilize the body. Our first-order analysis indicates that the bodies in Figures 12.14(b) and 12.14(c) can each rotate about their centers in the three-finger grasps, but in fact this is not possible for the body in Figure 12.14(b) – a second-order analysis would tell us that this body is actually immobilized. Finally, the first-order analysis tells us that the two-fingered grasps in Figures 12.14(d)–(f) are identical, but in fact the body in Figure 12.14(f) is immobilized by only two fingers owing to curvature effects.

To summarize, our first-order analysis always correctly labels breaking and penetrating motions but second- and higher-order effects may change first-order roll–slide motions to breaking or penetrating. If a body is in form closure by first-order analysis, it is in form closure for any analysis. If only roll-slide motions are feasible by first-order analysis, the body could be in form closure by a higher-order analysis; otherwise, the body is not in form closure by any analysis.

12.1.7.2 A Linear Programming Test for First-Order Form Closure

Let $F = [\mathcal{F}_1 \ \mathcal{F}_2 \ \cdots \ \mathcal{F}_j] \in \mathbb{R}^{n \times j}$ be a matrix whose columns are formed by the j contact wrenches. For spatial bodies, $n = 6$ and for planar bodies, $n = 3$ with $\mathcal{F}_i = [m_{iz} \ f_{ix} \ f_{iy}]^{\mathrm{T}}$. The contacts yield form closure if there exists a vector of weights $k \in \mathbb{R}^j$, $k \geq 0$, such that $Fk + \mathcal{F}_{\text{ext}} = 0$ for all $\mathcal{F}_{\text{ext}} \in \mathbb{R}^n$.

Clearly the body is not in form closure if the rank of F is not full ($\text{rank}(F) < n$). If F is full rank, the form-closure condition is equivalent to the existence of strictly positive coefficients $k > 0$ such that $Fk = 0$. We can formulate this test as the following set of conditions, which is an example of a **linear program**:

$$\begin{aligned} \text{find} \quad & k \\ \text{minimizing} \quad & \mathbf{1}^{\mathrm{T}} k \\ \text{such that} \quad & Fk = 0 \\ & k_i \geq 1, \ i = 1, \ldots, j, \end{aligned} \tag{12.14}$$

where $\mathbf{1}$ is a j-vector of ones. If F is full rank and there exists a solution k to (12.14), the body is in first-order form closure. Otherwise it is not. Note that the objective function $\mathbf{1}^{\mathrm{T}} k$ is not necessary to answer the binary question, depending on the LP solver, but it is included to make sure the problem is well posed.

Example 12.7. The planar body in Figure 12.15 has a hole in the center. Two fingers each touch two different edges of the hole, creating four contact normals. The matrix $F = [\mathcal{F}_1 \ \mathcal{F}_2 \ \mathcal{F}_3 \ \mathcal{F}_4]$ is given by

$$F = \begin{bmatrix} 0 & 0 & -1 & 2 \\ -1 & 0 & 1 & 0 \\ 0 & -1 & 0 & 1 \end{bmatrix}.$$

The matrix F is clearly rank 3. The linear program of (12.14) returns a solution with $k_1 = k_3 = 2$, $k_2 = k_4 = 1$, so with this grasp the body is in form closure. You could test this in MATLAB, for example, using the `linprog` function, which takes as arguments: the objective function, expressed as a vector of weights f

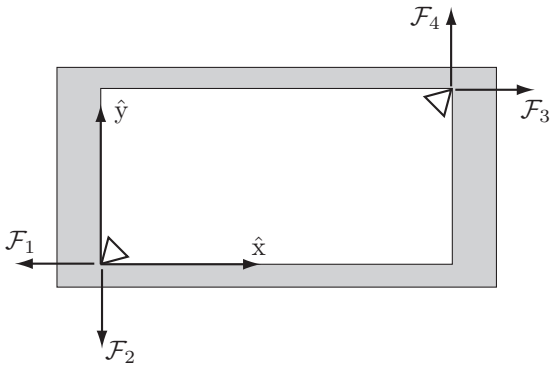

Figure 12.15: Two fingers grasping the interior of an object.

on the elements of k; a set of inequality constraints on k of the form $Ak \leq b$ (used to encode $k_i \geq 1$); and a set of equality constraints of the form $A_{\text{eq}}k = b_{\text{eq}}$ (used to encode $Fk = 0$);

```
f = [1,1,1,1];
A = [[-1,0,0,0]; [0,-1,0,0]; [0,0,-1,0]; [0,0,0,-1]];
b = [-1,-1,-1,-1];
F = [[0,0,-1,2]; [-1,0,1,0]; [0,-1,0,1]];  % the F matrix
Aeq = F;
beq = [0,0,0];
k = linprog(f,A,b,Aeq,beq);
```

which yields the result

```
k =
    2.0000
    1.0000
    2.0000
    1.0000
```

If the right-hand finger were moved to the bottom right corner of the hole, the new F matrix

$$F = \begin{bmatrix} 0 & 0 & 0 & -2 \\ -1 & 0 & 1 & 0 \\ 0 & -1 & 0 & -1 \end{bmatrix}$$

would still be full rank, but there would be no solution to the linear program. This grasp does not yield form closure: the body can slide downward on the page.

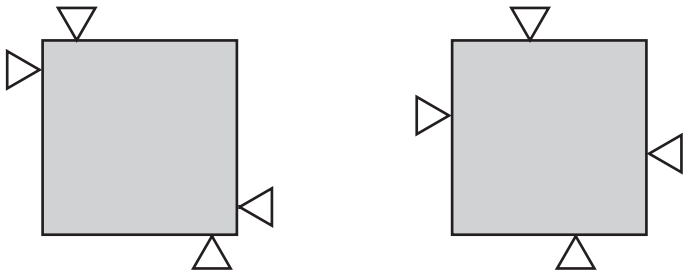

Figure 12.16: Both grasps yield form closure, but which is better?

12.1.7.3 Measuring the Quality of a Form-Closure Grasp

Consider the two form-closure grasps shown in Figure 12.16. Which is a better grasp?

Answering this question requires a metric measuring the quality of a grasp. A **grasp metric** takes the set of contacts $\{\mathcal{F}_i\}$ and returns a single value $\text{Qual}(\{\mathcal{F}_i\})$, where $\text{Qual}(\{\mathcal{F}_i\}) < 0$ indicates that the grasp does not yield form closure, and larger positive values indicate better grasps.

There are many reasonable choices of grasp metric. As an example, suppose that, to avoid damaging the body, we require that the magnitude of the force at contact i be less than or equal to $f_{i,\max} > 0$. Then the total set of contact wrenches that can be applied by the j contacts is given by

$$CF = \left\{ \sum_{i=1}^{j} f_i \mathcal{F}_i \;\middle|\; f_i \in [0, f_{i,\max}] \right\}. \tag{12.15}$$

See Figure 12.17 for an example in two dimensions. This shows the convex sets of wrenches that the contacts can apply to resist disturbance wrenches applied to the body. If the grasp yields form closure, the set includes the origin of the wrench space in its interior.

Now the problem is to turn this polytope into a single number representing the quality of the grasp. Ideally this process would use some idea of the disturbance wrenches that the body can be expected to experience. A simpler choice is to set $\text{Qual}(\{\mathcal{F}_i\})$ to be the radius of the largest ball of wrenches, centered at the origin of the wrench space, that fits inside the convex polytope. In evaluating this radius, two caveats should be considered: (1) moments and forces have different units, so there is no obvious way to equate force and moment magnitudes, and (2) the moments due to contact forces depend on the location of the space-frame origin. To address (1), it is common to choose a characteristic

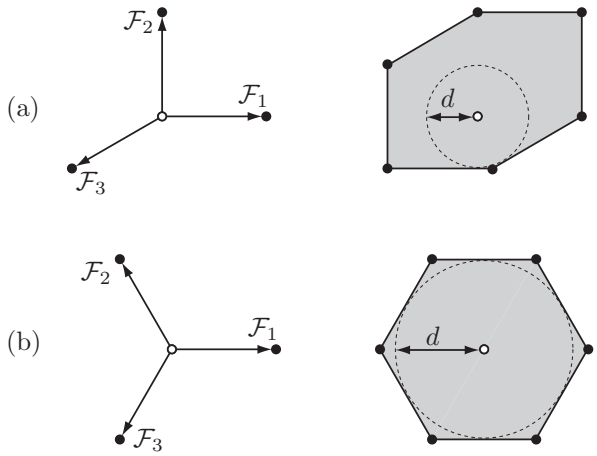

Figure 12.17: (a) A set of three contact wrenches in a two-dimensional wrench space, and the radius d of the largest ball of wrenches centered at the origin that fits inside the wrench polygon. (b) A different set of three wrenches yielding a larger inscribed ball.

length r of the grasped body and convert contact moments m to forces m/r. To address (2), the origin can be chosen somewhere near the geometric center of the body or at its center of mass.

Given the choice of the space frame and the characteristic length r, we simply calculate the signed distance from the origin of the wrench space to each hyperplane on the boundary of CF. The minimum of these distances is $\text{Qual}(\{\mathcal{F}_i\})$ (Figure 12.17).

Returning to our original example in Figure 12.16, we can see that if each finger is allowed to apply the same force then the grasp on the left may be considered better, as the contacts can resist greater moments about the center of the object.

12.1.7.4 Choosing Contacts for Form Closure

Many methods have been suggested for choosing form-closure contacts for fixturing or grasping. One approach is to sample candidate grasp points on the surface of the body (four for planar bodies or seven for spatial) until a set is found yielding form closure. From there, the candidate grasp points may be incrementally repositioned according to gradient ascent, using the grasp metric, i.e., $\partial\,\text{Qual}(p)/\partial p$, where p is the vector of all the coordinates of the contact

locations.[4]

12.2 Contact Forces and Friction

12.2.1 Friction

A commonly used model of friction in robotic manipulation is **Coulomb friction**. This experimental law states that the tangential friction force magnitude f_t is related to the normal force magnitude f_n by $f_t \leq \mu f_n$, where μ is called the **friction coefficient**. If the contact is sliding, or currently rolling but with incipient slip (i.e., at the next instant the contacts are sliding), then $f_t = \mu f_n$ and the direction of the friction force is opposite to that of the sliding direction, i.e., friction dissipates energy. The friction force is independent of the speed of sliding.

Often two friction coefficients are defined, a static friction coefficient μ_s and a kinetic (or sliding) friction coefficient μ_k, where $\mu_s \geq \mu_k$. This implies that a larger friction force is available to resist the initial motion but, once motion has begun, the resisting force is smaller. Many other friction models have been developed with different functional dependencies on factors such as the speed of sliding and the duration of static contact before sliding. All these are aggregate models of complex microscopic behavior. For simplicity, we will use the simplest Coulomb friction model with a single friction coefficient μ. This model is reasonable for hard, dry, materials. The friction coefficient depends on the two materials in contact and typically ranges from 0.1 to 1.

For a contact normal in the $+\hat{z}$-direction, the set of forces that can be transmitted through the contact satisfies

$$\sqrt{f_x^2 + f_y^2} \leq \mu f_z, \qquad f_z \geq 0. \tag{12.16}$$

Figure 12.18(a) shows that this set of forces forms a **friction cone**. The set of forces that the finger can apply to the plane lies inside the cone shown. Figure 12.18(b) shows the same cone from a side view, illustrating the **friction angle** $\alpha = \tan^{-1}\mu$, which is the half-angle of the cone. If the contact is not sliding, the force may be anywhere inside the cone. If the finger slides to the right, the force it applies lies on the right-hand edge of the friction cone, with magnitude determined by the normal force. Correspondingly, the plane applies the opposing force to the finger, and the direction of the tangential (frictional) portion of this force opposes the sliding direction.

[4] The gradient vector $\partial \,\mathrm{Qual}(p)/\partial p$ must be projected onto the tangent planes at the points of contact to keep the contact locations on the surface of the object.

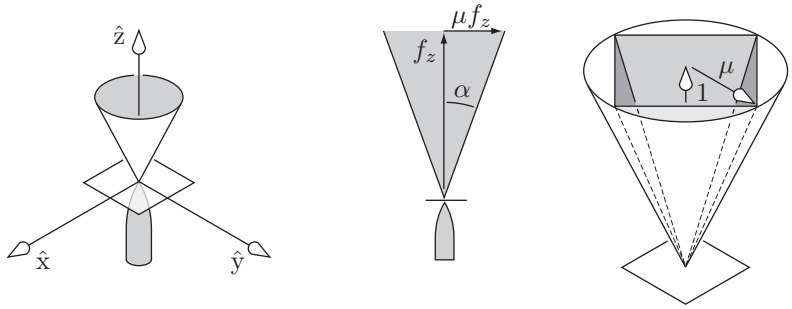

Figure 12.18: (a) A friction cone illustrating all possible forces that can be transmitted through the contact. (b) A side view of the same friction cone showing the friction coefficient μ and the friction angle $\alpha = \tan^{-1}\mu$. (c) An inscribed polyhedral convex cone approximation to the circular friction cone.

To allow linear formulations of contact mechanics problems, it is often convenient to represent the convex circular cone by a polyhedral convex cone. Figure 12.18(c) shows an inscribed four-sided pyramidal approximation of the friction cone, defined by the positive span of the (f_x, f_y, f_z) cone edges $(\mu, 0, 1)$, $(-\mu, 0, 1)$, $(0, \mu, 1)$, and $(0, -\mu, 1)$. We can obtain a tighter approximation to the circular cone by using more edges. An inscribed cone underestimates the friction forces available, while a circumscribed cone overestimates the friction forces. The choice of which to use depends on the application. For example, if we want to ensure that a robot hand can grasp an object, it is a good idea to underestimate the friction forces available.

For planar problems, no approximation is necessary – a friction cone is exactly represented by the positive span of the two edges of the cone, similarly to the side view illustrated in Figure 12.18(b).

Once we choose a coordinate frame, any contact force can be expressed as a wrench $\mathcal{F} = ([p]f, f)$, where p is the contact location. This turns a friction cone into a wrench cone. A planar example is shown in Figure 12.19. The two edges of the planar friction cone give two rays in the wrench space, and the wrenches that can be transmitted to the body through the contact give the positive span of basis vectors along these edges. If $\mathcal{F}_1$ and $\mathcal{F}_2$ are basis vectors for these wrench cone edges, we write the wrench cone as $\mathcal{WC} = \text{pos}(\{\mathcal{F}_1, \mathcal{F}_2\})$.

If multiple contacts act on a body, then the total set of wrenches that can be transmitted to the body through the contacts is the positive span of all the

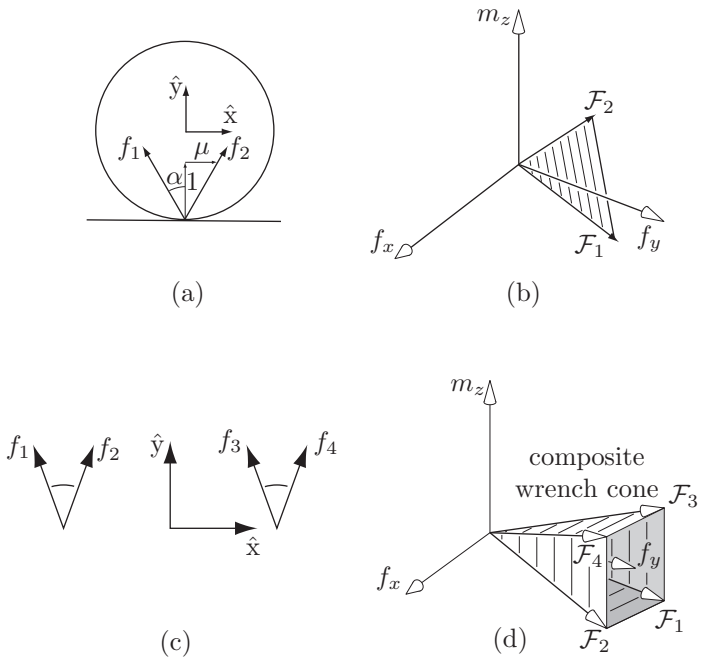

Figure 12.19: (a) A planar friction cone with friction coefficient μ and corresponding friction angle $\alpha = \tan^{-1}\mu$. (b) The corresponding wrench cone. (c) Two friction cones. (d) The corresponding composite wrench cone.

individual wrench cones $\mathcal{WC}_i$,

$$\mathcal{WC} = \text{pos}(\{\mathcal{WC}_i\}) = \left\{ \sum_i k_i \mathcal{F}_i \;\middle|\; \mathcal{F}_i \in \mathcal{WC}_i, k_i \geq 0 \right\}.$$

This composite wrench cone is a convex cone rooted at the origin. An example of such a composite wrench cone is shown in Figure 12.19(d) for a planar body with the two friction cones shown in Figure 12.19(c). For planar problems, the composite wrench cone in the three-dimensional wrench space is polyhedral. For spatial problems, wrench cones in the six-dimensional wrench space are not polyhedral unless the individual friction cones are approximated by polyhedral cones, as in Figure 12.18(c).

If a contact or set of contacts acting on a body is ideally force-controlled, the wrench $\mathcal{F}_{\text{cont}}$ specified by the controller must lie within the composite wrench

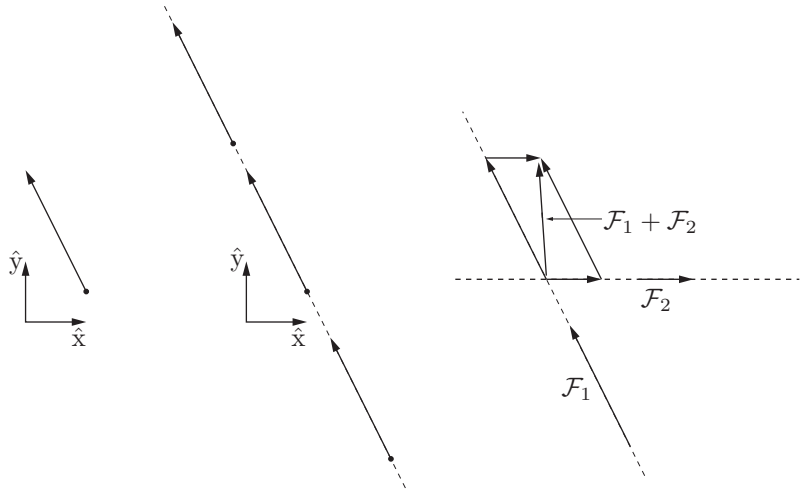

Figure 12.20: (Left) The planar wrench $\mathcal{F} = (m_z, f_x, f_y) = (2.5, -1, 2)$ represented as an arrow in the x̂–ŷ-plane. (Middle) The same wrench can be represented by an arrow anywhere along the line of action. (Right) Two wrenches are summed by sliding their arrows along their lines of action until the bases of the arrows are coincident, then doing a vector sum by the parallelogram construction.

cone corresponding to those contacts. If there are other non-force-controlled contacts acting on the body, then the cone of possible wrenches on the body is equivalent to the wrench cone from the non-force-controlled contacts but translated to be rooted at $\mathcal{F}_{\text{cont}}$.

12.2.2 Planar Graphical Methods

12.2.2.1 Representing Wrenches

Any planar wrench $\mathcal{F} = (m_z, f_x, f_y)$ with a nonzero linear component can be represented as an arrow drawn in the plane, where the base of the arrow is at the point

$$(x, y) = \frac{1}{f_x^2 + f_y^2}(m_z f_y, -m_z f_x)$$

and the head of the arrow is at $(x + f_x, y + f_y)$. The moment is unchanged if we slide the arrow anywhere along its line, so any arrow of the same direction and length along this line represents the same wrench (Figure 12.20). If $f_x = f_y = 0$

and $m_z \neq 0$, the wrench is a pure moment, and we do not try to represent it graphically.

Two wrenches, represented as arrows, can be summed graphically by sliding the arrows along their lines until the bases of the arrows are coincident. The arrow corresponding to the sum of the two wrenches is obtained as shown in Figure 12.20. The approach can be applied sequentially to sum multiple wrenches represented as arrows.

12.2.2.2 Representing Wrench Cones

In the previous section each wrench had a specified magnitude. However, a rigid-body contact implies that the contact normal force can be arbitrarily large; the normal force achieves the magnitude needed to prevent two bodies from penetrating. Therefore it is useful to have a representation of all wrenches of the form $k\mathcal{F}$, where $k \geq 0$ and $\mathcal{F} \in \mathbb{R}^3$ is a basis vector.

One such representation is **moment labeling**. The arrow for the basis wrench $\mathcal{F}$ is drawn as described in Section 12.2.2.1. Then all points in the plane to the left of the line of the arrow are labeled '+', indicating that any positive scaling of $\mathcal{F}$ creates a positive moment m_z about those points, and all points in the plane to the right of the arrow are labeled '−', indicating that any positive scaling of $\mathcal{F}$ creates a negative moment about those points. Points on the line are labeled '±'.

Generalizing, moment labels can represent any homogeneous convex planar wrench cone, much as a homogeneous convex planar twist cone can be represented as a convex CoR region. Given a collection of directed force lines corresponding to wrenches $k_i\mathcal{F}_i$ for all $k_i \geq 0$, the wrench cone $\text{pos}(\{\mathcal{F}_i\})$ can be represented by labeling each point in the plane with a '+' if each $\mathcal{F}_i$ makes a nonnegative moment about that point, with a '−' if each $\mathcal{F}_i$ makes a nonpositive moment about that point, with a '±' if each $\mathcal{F}_i$ makes zero moment about that point, or with a blank label if at least one wrench makes a positive moment and at least one wrench makes a negative moment about that point.

The idea is best illustrated by an example. In Figure 12.21(a), the basis wrench $\mathcal{F}_1$ is represented by labeling the points to the left of the force line with a '+' and points to the right of the line with a '−'. Points on the line are labeled '±'. In Figure 12.21(b), another basis wrench is added, which could represent the other edge of a planar friction cone. Only the points in the plane that are consistently labeled for both lines of force retain their labels; inconsistently labeled points lose their labels. Finally, a third basis wrench is added in Figure 12.21(c). The result is a single region labeled '+'. A nonnegative linear combination of the three basis wrenches can create any line of force in the plane

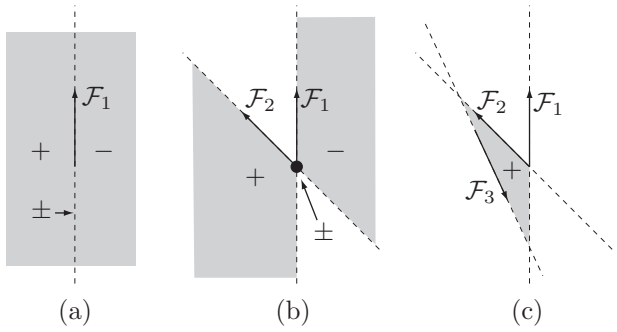

Figure 12.21: (a) Representing a line of force by moment labels. (b) Representing the positive span of two lines of force by moment labels. (c) The positive span of three lines of force.

that passes around this region in a counterclockwise sense. No other wrench can be created.

If an additional basis wrench were added passing clockwise around the region labeled '+' in Figure 12.21(c), then there would be no consistently labeled point in the plane; the positive linear span of the four wrenches would be the entire wrench space $\mathbb{R}^3$.

The moment-labeling representation is equivalent to a homogeneous convex wrench cone representation. The moment-labeling regions in each part, (a), (b) and (c), of Figure 12.21 are properly interpreted as a single convex region, much like the CoR regions of Section 12.1.6.

12.2.3 Force Closure

Consider a single movable body and a number of frictional contacts. We say the contacts result in **force closure** if the composite wrench cone contains the entire wrench space, so that any external wrench $\mathcal{F}_{\text{ext}}$ on the body can be balanced by contact forces.

We can derive a simple linear test for force closure which is exact for planar cases and approximate for spatial cases. Let $\mathcal{F}_i$, $i = 1, \ldots, j$, be the wrenches corresponding to the edges of the friction cones for all the contacts. For planar problems, each friction cone contributes two edges and, for spatial problems, each friction cone contributes three or more edges, depending on the polyhedral approximation chosen (see Figure 12.18(c)). The columns of an $n \times j$ matrix F are the $\mathcal{F}_i$, where $n = 3$ for planar problems and $n = 6$ for spatial problems.

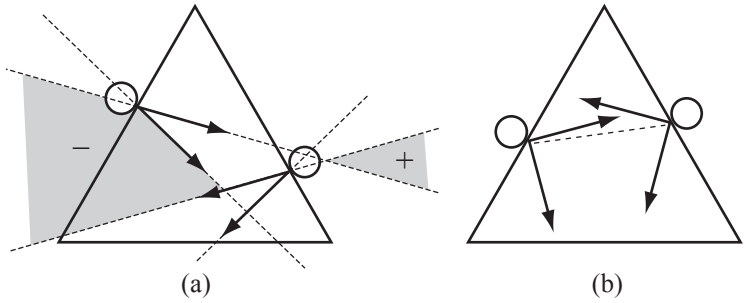

Figure 12.22: An equilateral triangle can be force-closure-grasped by two fingers on the edges of the triangle if $\mu \geq \tan 30^\circ \approx 0.577$. (a) The grasp shown with $\mu = 0.25$ would not be in force closure, as indicated by the consistently labeled moment-labeling region. (b) The grasp shown is in force closure with $\mu = 1$; the dashed line indicates that the two contacts can "see" each other, i.e., their line of sight is inside both friction cones.

Now, the test for force closure is identical to that for form closure. The contacts yield force closure if

- rank $F = n$, and
- there exists a solution to the linear programming problem (12.14).

In the case of $\mu = 0$, each contact can provide forces only along the normal direction, and force closure is equivalent to first-order form closure.

12.2.3.1 Number of Contacts Needed for Force Closure

For planar problems, four contact wrenches are sufficient to positively span the three-dimensional wrench space, which means that as few as two frictional contacts (with two friction cone edges each) are sufficient for force closure. Using moment labeling, we see that force closure is equivalent to having no consistent moment labels. For example, if the two contacts can "see" each other by a line of sight inside both friction cones, we have force closure (Figure 12.22(b)).

It is important to note that force closure simply means that the contact friction cones can generate any wrench. It does not necessarily mean that the body will not move in the presence of an external wrench. For the example of Figure 12.22(b), whether the triangle falls under gravity depends on the internal forces between the fingers. If the motors powering the fingers cannot provide sufficient forces, or if they are restricted to generate forces only in certain directions, the triangle may fall despite force closure.

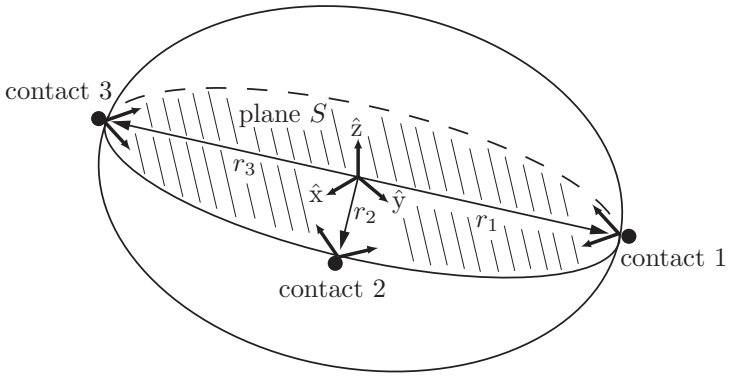

Figure 12.23: A spatial rigid body restrained by three point contacts with friction.

Two frictional point contacts are insufficient to yield force closure for spatial bodies, as there is no way to generate a moment about the axis joining the two contacts. A force-closure grasp can be obtained with as few as three frictional contacts, however. A particularly simple and appealing result due to [89] reduces the force-closure analysis of spatial frictional grasps to a planar force-closure problem. Referring to Figure 12.23, suppose that a rigid body is constrained by three frictional point contacts. If the three contact points happen to be collinear then obviously any moment applied about this line cannot be resisted by the three contacts. We can therefore exclude this case and assume that the three contact points are not collinear. The three contacts then define a unique plane S and, at each contact point, three possibilities arise (see Figure 12.24):

- the friction cone intersects S in a planar cone;
- the friction cone intersects S in a line;
- the friction cone intersects S at a point.

The body is in force closure if and only if each friction cone intersects S in a planar cone and S is also in planar force closure.

Theorem 12.8. *Given a spatial rigid body restrained by three point contacts with friction, the body is in force closure if and only if the friction cone at each contact intersects the plane S of the contacts in a cone and the plane S is in planar force closure.*

Proof. First, the necessity condition – if the spatial rigid body is in force closure then each friction cone intersects S in a planar cone and S is also in planar force

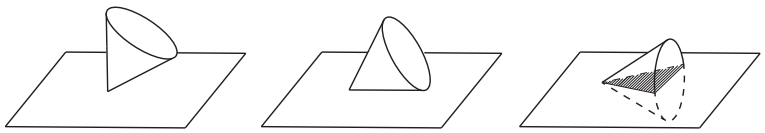

Figure 12.24: Three possibilities for the intersection between a friction cone and a plane.

closure – is easily verified: if the body is in spatial force closure then S (which is a part of the body) must also be in planar force closure. Moreover, if even one friction cone intersects S in a line or point then there will be external moments (e.g., about the line between the remaining two contact points) that cannot be resisted by the grasp.

To prove the sufficiency condition – if each friction cone intersects S in a planar cone and S is also in planar force closure then the spatial rigid body is in force closure – choose a fixed reference frame such that S lies in the $\hat{x}$–$\hat{y}$-plane and let $r_i \in \mathbb{R}^3$ denote the vector from the fixed-frame origin to contact point i (see Figure 12.23). Denoting the contact force at i by $f_i \in \mathbb{R}^3$, the contact wrench $\mathcal{F}_i \in \mathbb{R}^6$ is then of the form

$$\mathcal{F}_i = \begin{bmatrix} m_i \\ f_i \end{bmatrix}, \tag{12.17}$$

where each $m_i = r_i \times f_i$, $i = 1, 2, 3$. Denote the arbitrary external wrench $\mathcal{F}_{\text{ext}} \in \mathbb{R}^6$ by

$$\mathcal{F}_{\text{ext}} = \begin{bmatrix} m_{\text{ext}} \\ f_{\text{ext}} \end{bmatrix} \in \mathbb{R}^6. \tag{12.18}$$

Force closure then requires that there exist contact wrenches $\mathcal{F}_i$, $i = 1, 2, 3$, each lying inside its respective friction cone, such that, for any external disturbance wrench $\mathcal{F}_{\text{ext}}$, the following equality is satisfied:

$$\mathcal{F}_1 + \mathcal{F}_2 + \mathcal{F}_3 + \mathcal{F}_{\text{ext}} = 0 \tag{12.19}$$

or, equivalently,

$$f_1 + f_2 + f_3 + f_{\text{ext}} = 0, \tag{12.20}$$

$$(r_1 \times f_1) + (r_2 \times f_2) + (r_3 \times f_3) + m_{\text{ext}} = 0. \tag{12.21}$$

If each contact force and moment, as well as the external force and moment, is orthogonally decomposed into components lying on the plane spanned by S (corresponding to the $\hat{x}$–$\hat{y}$-plane in our chosen reference frame) and its normal

subspace N (corresponding to the $\hat{z}$-axis in our chosen reference frame) then the previous force-closure equalities can be written as

$$\begin{aligned} f_{1S} + f_{2S} + f_{3S} &= -f_{\text{ext},S}, && (12.22)\\ (r_1 \times f_{1S}) + (r_2 \times f_{2S}) + (r_3 \times f_{3S}) &= -m_{\text{ext},S}, && (12.23)\\ f_{1N} + f_{2N} + f_{3N} &= -f_{\text{ext},N}, && (12.24)\\ (r_1 \times f_{1N}) + (r_2 \times f_{2N}) + (r_3 \times f_{3N}) &= -m_{\text{ext},N}. && (12.25) \end{aligned}$$

In what follows we shall use S to refer both to the slice of the rigid body corresponding to the $\hat{x}$–$\hat{y}$-plane and to the $\hat{x}$–$\hat{y}$-plane itself; we will always identify N with the $\hat{z}$-axis.

Proceeding with the proof of sufficiency, we now show that if S is in planar force closure then the body is in spatial force closure. In terms of Equations (12.24) and (12.25) we wish to show that, for any arbitrary forces $f_{\text{ext},S} \in S$, $f_{\text{ext},N} \in N$ and arbitrary moments $m_{\text{ext},S} \in S$, $m_{\text{ext},N} \in N$, there exist contact forces $f_{iS} \in S$, $f_{iN} \in N$, $i = 1, 2, 3$, that satisfy (12.24) and(12.25) such that, for each $i = 1, 2, 3$, the contact force $f_i = f_{iS} + f_{iN}$ lies in friction cone i.

First consider the force-closure equations (12.24) and (12.25) in the normal direction N. Given an arbitrary external force $f_{\text{ext},N} \in N$ and external moment $m_{\text{ext},S} \in S$, Equations (12.24) and (12.25) constitute a set of three linear equations in three unknowns. From our assumption that the three contact points are never collinear, these equations will always have a unique solution set $\{f_{1N}^*, f_{2N}^*, f_{3N}^*\}$ in N.

Since S is assumed to be in planar force closure, for any arbitrary $f_{\text{ext},S} \in S$ and $m_{\text{ext},N} \in N$ there will exist planar contact forces $f_{iS} \in S$, $i = 1, 2, 3$, that lie inside their respective planar friction cones and also satisfy Equations (12.22) and (12.23). This solution set is not unique: one can always find a set of internal forces $\eta_i \in S$, $i = 1, 2, 3$, each lying inside its respective friction cone, satisfying

$$\begin{aligned} \eta_1 + \eta_2 + \eta_3 &= 0, && (12.26)\\ (r_1 \times \eta_1) + (r_2 \times \eta_2) + (r_3 \times \eta_3) &= 0. && (12.27) \end{aligned}$$

(To see why such η_i exist, recall that since S is assumed to be in planar force closure, solutions to (12.22) and (12.23) must exist for $f_{\text{ext},S} = \mu_{\text{ext},N} = 0$; these solutions are precisely the internal forces η_i). Note that these two equations constitute three linear equality constraints involving six variables, so that there exists a three-dimensional linear subspace of solutions for $\{\eta_1, \eta_2, \eta_3\}$.

Now, if $\{f_{1S}, f_{2S}, f_{3S}\}$ satisfy (12.22) and (12.23) then so will $\{f_{1S}+\eta_1, f_{2S}+\eta_2, f_{3S}+\eta_3\}$. The internal forces $\{\eta_1, \eta_2, \eta_3\}$ can, in turn, be chosen to have

sufficiently large magnitudes that the contact forces

$$f_1 = f_{1N}^* + f_{1S} + \eta_1, \quad (12.28)$$
$$f_2 = f_{2N}^* + f_{2S} + \eta_2, \quad (12.29)$$
$$f_3 = f_{3N}^* + f_{3S} + \eta_3 \quad (12.30)$$

all lie inside their respective friction cones. This completes the proof of the sufficiency condition. □

12.2.3.2 Measuring the Quality of a Force-Closure Grasp

Friction forces are not always repeatable. For example, try putting a coin on a book and tilting the book. The coin should begin to slide when the book is at an angle $\alpha = \tan^{-1}\mu$ with respect to the horizontal. If you do the experiment several times then you may find a range of measured values of μ, owing to effects that are difficult to model. For that reason, when choosing between grasps it is reasonable to choose finger locations that minimize the friction coefficient needed to achieve force closure.

12.2.4 Duality of Force and Motion Freedoms

Our discussion of kinematic constraints and friction should have made it apparent that, for any point contact and contact label, the number of equality constraints on a body's motion caused by that contact is equal to the number of wrench freedoms it provides. For example, a breaking contact `B` provides zero equality constraints on the body's motion and also allows no contact force. A fixed contact `R` provides three motion constraints (the motion of a point on the body is specified) and three freedoms in the contact force: any wrench in the interior of the contact wrench cone is consistent with the contact mode. Finally, a slipping contact `S` provides one equality motion constraint (one equation on the body's motion must be satisfied to maintain the contact) and, for a given motion satisfying the constraint, the contact wrench has only one freedom: the magnitude of the contact wrench on the edge of the friction cone and opposing the slipping direction. In the planar case, the motion constraints and wrench freedoms for `B`, `S`, and `R` contacts are 0, 1, and 2, respectively.

12.3 Manipulation

So far we have studied the feasible twists and contact forces due to a set of contacts. We have also considered two types of manipulation: form-closure and force-closure grasping.

Manipulation consists of much more than just grasping, however. It includes almost anything where manipulators impose motions or forces with the purpose of achieving the motion or restraint of objects. Examples include carrying glasses on a tray without toppling them, pivoting a refrigerator about one of its feet, pushing a sofa along the floor, throwing and catching a ball, transporting parts on a vibratory conveyor, etc. Endowing a robot with methods of manipulation beyond grasp-and-carry allows it to manipulate several parts simultaneously, manipulate parts that are too large to be grasped or too heavy to be lifted, or even to send parts outside the workspace of the end-effector by throwing them.

To plan such manipulation tasks, we use the contact kinematic constraints of Section 12.1, the Coulomb friction law of Section 12.2, and the dynamics of rigid bodies. Restricting ourselves to a single rigid body and using the notation of Chapter 8, the body's dynamics are written as

$$\mathcal{F}_{\text{ext}} + \sum k_i \mathcal{F}_i = \mathcal{G}\dot{\mathcal{V}} - [\text{ad}_{\mathcal{V}}]^{\text{T}} \mathcal{G}\mathcal{V}, \qquad k_i \geq 0, \quad \mathcal{F}_i \in \mathcal{WC}_i, \tag{12.31}$$

where $\mathcal{V}$ is the body's twist, $\mathcal{G}$ is its spatial inertia matrix, $\mathcal{F}_{\text{ext}}$ is the external wrench acting on the body due to gravity, etc., $\mathcal{WC}_i$ is the set of possible wrenches acting on the body due to contact i, and $\sum k_i \mathcal{F}_i$ is the wrench due to the contacts. All wrenches are written in the body's center-of-mass frame. Now, given a set of motion- or force-controlled contacts acting on the body, and the initial state of the system, one method for solving for the motion of the body is the following.

(a) Enumerate the set of possible contact modes considering the current state of the system (e.g., a contact that is currently sticking can transition to sliding or breaking). The contact modes consist of the contact labels `R`, `S`, and `B` at each contact.

(b) For each contact mode, determine whether there exists a contact wrench $\sum k_i \mathcal{F}_i$ that is consistent with the contact mode and Coulomb's law, and an acceleration $\dot{\mathcal{V}}$ consistent with the kinematic constraints of the contact mode, such that Equation (12.31) is satisfied. If so, this contact mode, contact wrench, and body acceleration comprises a consistent solution to the rigid-body dynamics.

This kind of "case analysis" may sound unusual; we are not simply solving a set of equations. It also leaves open the possibility that we could find more than one consistent solution, or perhaps no consistent solution. This is, in fact, the case: we can define problems with multiple solutions (**ambiguous** problems) and problems with no solutions (**inconsistent** problems). This state of affairs

is a bit unsettling; surely there is exactly one solution to any real mechanics problem! But this is the price we pay for using the assumptions of perfectly rigid bodies and Coulomb friction. Despite the possibility of zero or multiple solutions, for many problems the method described above will yield a unique contact mode and motion.

Some of the manipulation tasks below are **quasistatic**, where the velocities and accelerations of the bodies are small enough that inertial forces may be ignored. Contact wrenches and external wrenches are always in force balance, and Equation (12.31) reduces to

$$\mathcal{F}_{\text{ext}} + \sum k_i \mathcal{F}_i = 0, \qquad k_i \geq 0, \quad \mathcal{F}_i \in \mathcal{WC}_i. \tag{12.32}$$

Below we illustrate the methods of this chapter with four examples.

Example 12.9 (A block carried by two fingers)**.** Consider a planar block in gravity supported by two fingers, as in Figure 12.25(a). The friction coefficient between one finger and the block is $\mu = 1$, and the other contact is frictionless. Thus the cone of wrenches that can be applied by the fingers is $\text{pos}(\{\mathcal{F}_1, \mathcal{F}_2, \mathcal{F}_3\})$, as shown using moment labeling in Figure 12.25(b).

Our first question is whether the stationary fingers can keep the block at rest. To do so, the fingers must provide a wrench $\mathcal{F} = (m_z, f_x, f_y) = (0, 0, \mathfrak{m}g)$ to balance the wrench $\mathcal{F}_{\text{ext}} = (0, 0, -\mathfrak{m}g)$ due to gravity, where $g > 0$. As shown in Figure 12.25(b), this wrench is not in the composite cone of possible contact wrenches. Therefore the contact mode `RR` is not feasible, and the block will move relative to the fingers.

Now consider the case where the fingers each accelerate to the left at $2g$. In this case the contact mode `RR` requires that the block also accelerate to the left at $2g$. The wrench needed to cause this acceleration is $(0, -2\mathfrak{m}g, 0)$. Therefore the total wrench that the fingers must apply to the block is $(0, -2\mathfrak{m}g, 0) - \mathcal{F}_{\text{ext}} = (0, -2\mathfrak{m}g, \mathfrak{m}g)$. As shown in Figures 12.25(c), (d), this wrench lies inside the composite wrench cone. Thus `RR` (the block stays stationary relative to the fingers) is a solution as the fingers accelerate to the left at $2g$.

This is called a **dynamic grasp** – inertial forces are used to keep the block pressed against the fingers while the fingers move. If we plan to manipulate the block using a dynamic grasp then we should make certain that no contact modes other than `RR` are feasible, for completeness.

Moment labels are convenient for understanding this problem graphically, but we can also solve it algebraically. The lower finger contacts the block at $(x, y) = (-3, -1)$ and the upper finger contacts the block at $(1, 1)$. This gives the basis contact wrenches

$$\mathcal{F}_1 = \frac{1}{\sqrt{2}}(-4, -1, 1), \quad \mathcal{F}_2 = \frac{1}{\sqrt{2}}(-2, 1, 1), \quad \mathcal{F}_3 = (1, -1, 0).$$

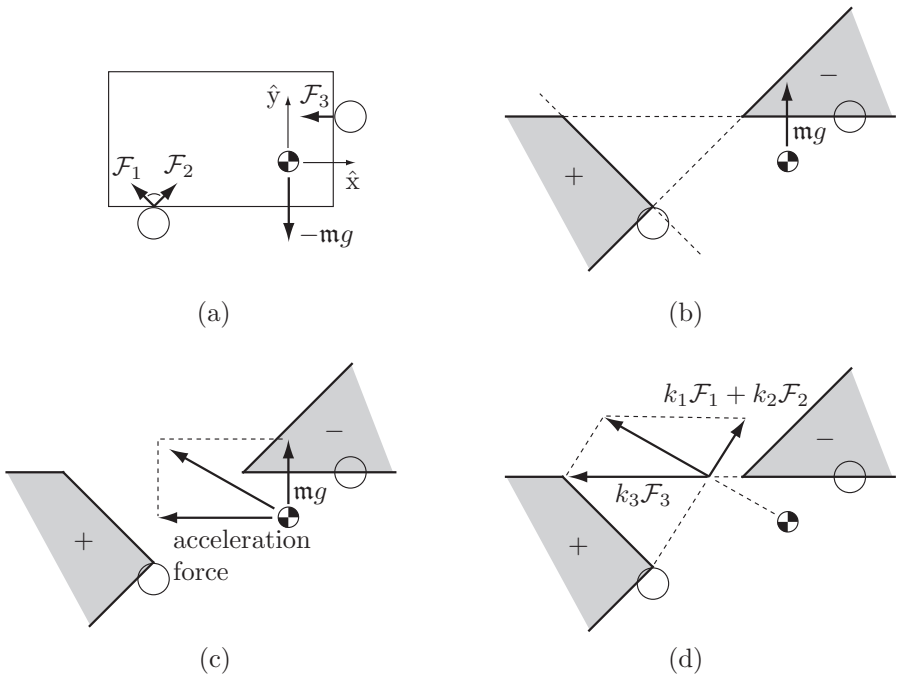

Figure 12.25: (a) A planar block in gravity supported by two robot fingers, the lower with a friction cone with $\mu = 1$ and the upper with $\mu = 0$. (b) The composite wrench cone that can be applied by the fingers represented using moment labels. To balance the block against gravity, the fingers must apply the line of force shown. This line has a positive moment with respect to points labeled '$-$', and therefore it cannot be generated by the two fingers. (c) For the block to match the fingers' acceleration to the left, the contacts must apply the vector sum of the wrench to balance gravity and the wrench needed to accelerate the block to the left. This total wrench lies inside the composite wrench cone, as the line of force has a positive moment with respect to points labeled '$+$' and a negative moment with respect to points labeled '$-$'. (d) The total wrench applied by the fingers in (c) can be translated along the line of action without changing the wrench. This allows us to visualize easily the components $k_1\mathcal{F}_1 + k_2\mathcal{F}_2$ and $k_3\mathcal{F}_3$ provided by the fingers.

Let the fingers' acceleration in the $\hat{\text{x}}$-direction be written a_x. Then, under the assumption that the block stays fixed with respect to the fingers (`RR` contact mode), Equation (12.31) can be written

$$k_1\mathcal{F}_1 + k_2\mathcal{F}_2 + k_3\mathcal{F}_3 + (0, 0, -\mathfrak{m}g) = (0, \mathfrak{m}a_x, 0). \tag{12.33}$$

This yields three equations in the three unknowns, k_1, k_2, k_3. Solving, we get

$$k_1 = -\frac{1}{2\sqrt{2}}(a_x + g)\mathfrak{m}, \qquad k_2 = \frac{1}{2\sqrt{2}}(a_x + 5g)\mathfrak{m}, \qquad k_3 = -\frac{1}{2}(a_x - 3g)\mathfrak{m}.$$

For the k_i to be nonnegative, we need $-5g \leq a_x \leq -g$. For $\hat{\mathrm{x}}$-direction finger accelerations in this range, a dynamic grasp is a consistent solution.

Example 12.10 (The meter-stick trick)**.** Try this experiment. Get a meter stick (or any similar long smooth stick) and balance it horizontally on your two index fingers. Place your left finger near the 10 cm mark and your right finger near the 60 cm mark. The center of mass is closer to your right finger but still between your fingers, so that the stick is supported. Now, keeping your left finger stationary, slowly move your right finger towards your left until they touch. What happens to the stick?

If you didn't try the experiment, you might guess that your right finger passes under the center of mass of the stick, at which point the stick falls. If you did try the experiment, you saw something different. Let's see why.

Figure 12.26 shows the stick supported by two frictional fingers. Since all motions are slow, we use the quasistatic approximation that the stick's acceleration is zero and so the net contact wrench must balance the gravitational wrench. As the two fingers move together, the stick must slip on one or both fingers to accommodate the fact that the fingers are getting closer to each other. Figure 12.26 shows the moment-labeling representation of the composite wrench cone for three different contact modes: `RSr`, where the stick remains stationary relative to the left finger and slips to the right relative to the right finger; `SlR`, where the stick slips to the left relative to the left finger and remains stationary relative to the right finger; and `SlSr`, where the stick slips on both fingers. It is clear from the figure that only the `SlR` contact mode can provide a wrench that balances the gravitational wrench. In other words, the right finger, which supports more of the stick's weight, remains fixed relative to the stick while the left finger slides under the stick. Since the right finger is moving to the left in the world frame, this means that the center of mass is moving to the left at the same speed. This continues until the center of mass is halfway between the fingers, at which point the stick transitions to the `SlSr` contact mode, and the center of mass stays centered between the fingers until they meet. The stick never falls.

Note that this analysis relies on the quasistatic assumption. It is easy to make the stick fall if you move your right finger quickly; the friction force at the right finger is not large enough to create the large stick acceleration needed to maintain a sticking contact. Also, in your experiment, you might notice that,

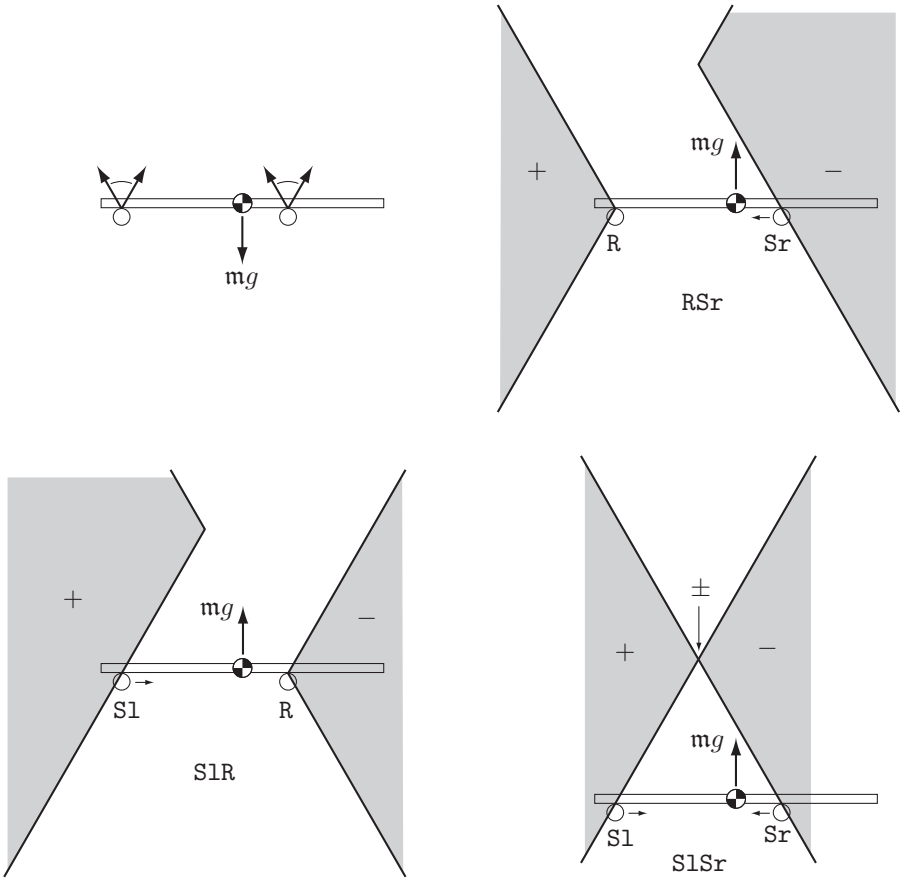

Figure 12.26: Top left: Two frictional fingers supporting a meter stick in gravity. The other three panels show the moment labels for the `RSr`, `SlR`, and `SlSr` contact modes. Only the `SlR` contact mode yields force balance.

when the center of mass is nearly centered, the stick does not actually achieve the idealized `SlSr` contact mode, but instead switches rapidly between the `SlR` and `RSr` contact modes. This occurs because the static friction coefficient is larger than the kinetic friction coefficient.

Example 12.11 (Stability of an assembly)**.** Consider the arch in Figure 12.27. Is it stable under gravity?

For a problem like this, graphical planar methods are difficult to use, since

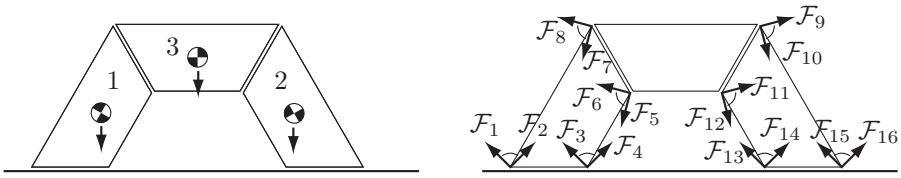

Figure 12.27: (Left) An arch under gravity. (Right) The friction cones at the contacts of stone 1 and the contacts of stone 2.

there are potentially multiple moving bodies. Instead we test algebraically for consistency of the contact mode with all contacts labeled `R`. The friction cones are shown in Figure 12.27. With these labelings of the friction cone edges, the arch can remain standing if there is a consistent solution if there exist $k_i \geq 0$ for $i = 1, \ldots, 16$ satisfying the following nine wrench-balance equations, three for each body:

$$\sum_{i=1}^{8} k_i \mathcal{F}_i + \mathcal{F}_{\text{ext1}} = 0,$$
$$\sum_{i=9}^{16} k_i \mathcal{F}_i + \mathcal{F}_{\text{ext2}} = 0,$$
$$-\sum_{i=5}^{12} k_i \mathcal{F}_i + \mathcal{F}_{\text{ext3}} = 0,$$

where $\mathcal{F}_{\text{ext}i}$ is the gravitational wrench on body i. The last set of equations comes from the fact that the wrenches that body 1 applies to body 3 are equal and opposite those that body 3 applies to body 1, and similarly for bodies 2 and 3.

This linear constraint satisfaction problem can be solved by a variety of methods, including linear programming.

Example 12.12 (Peg insertion)**.** Figure 12.28 shows a force-controlled planar peg in two-point contact with a hole during insertion. Also shown are the contact friction cones acting on the peg and the corresponding composite wrench cone, illustrated using moment labels. If the force controller applies the wrench $\mathcal{F}_1$ to the peg, it may jam – the hole may generate contact forces that balance $\mathcal{F}_1$. Therefore the peg may get stuck in this position. If the force controller applies the wrench $\mathcal{F}_2$, however, the contacts cannot balance the wrench and insertion proceeds.

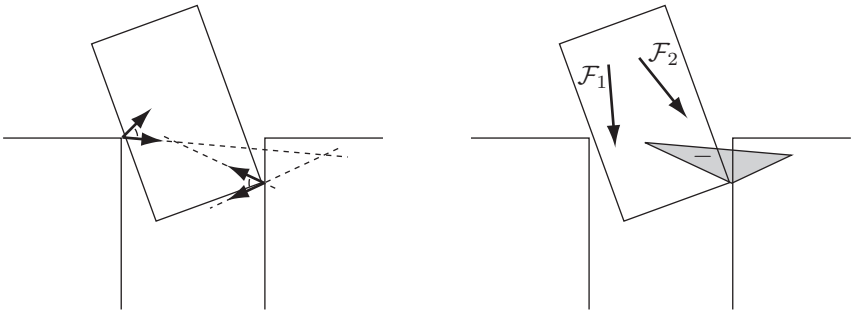

Figure 12.28: (Left) A peg in two-point contact with a hole. (Right) The wrench $\mathcal{F}_1$ may cause the peg to jam, while the wrench $\mathcal{F}_2$ continues to push the peg into the hole.

If the friction coefficients at the two contacts are large enough that the two friction cones "see" each other's base (Figure 12.22(b)), the peg is in force closure and the contacts may be able to resist any wrench (depending on the internal force between the two contacts). The peg is said to be wedged.

12.4 Summary

- Three ingredients are needed to solve rigid-body contact problems with friction: (1) the contact kinematics, which describes the feasible motions of rigid bodies in contact; (2) a contact force model, which describes the forces that can be transmitted through frictional contacts; and (3) rigid-body dynamics, as described in Chapter 8.
- Let two rigid bodies, A and B, be in point contact at p_A in a space frame. Let $\hat{n} \in \mathbb{R}^3$ be the unit contact normal, pointing into body A. Then the spatial contact wrench $\mathcal{F}$ associated with a unit force along the contact normal is $\mathcal{F} = [([p_A]\hat{n})^{\mathrm{T}} \; \hat{n}^{\mathrm{T}}]^{\mathrm{T}}$. The impenetrability constraint is
$$\mathcal{F}^{\mathrm{T}}(\mathcal{V}_A - \mathcal{V}_B) \geq 0,$$
where $\mathcal{V}_A$ and $\mathcal{V}_B$ are the spatial twists of A and B.
- A contact that is sticking or rolling is assigned the contact label `R`, a contact that is sliding is assigned the contact label `S`, and a contact that is breaking free is assigned the contact label `B`. For a body with multiple contacts, the contact mode is the concatenation of the labels of the individual contacts.

- A single rigid body subjected to multiple stationary point contacts has a homogeneous (rooted-at-the-origin) polyhedral convex cone of twists that satisfy all the impenetrability constraints.
- A homogeneous polyhedral convex cone of planar twists in $\mathbb{R}^3$ can be equivalently represented by a convex region of signed rotation centers in the plane.
- If a set of stationary contacts prevents a body from moving, purely by a kinematic analysis considering only the contact normals, the body is said to be in first-order form closure. The contact wrenches $\mathcal{F}_i$ for contacts $i = 1, \ldots, j$ positively span $\mathbb{R}^n$, where $n = 3$ for the planar case and $n = 6$ for the spatial case.
- At least four point contacts are required for first-order form closure of a planar body, and at least seven point contacts are required for first-order form closure of a spatial body.
- The Coulomb friction law states that the tangential frictional force magnitude f_t at a contact satisfies $f_\mathrm{t} \leq \mu f_\mathrm{n}$, where μ is the friction coefficient and f_n is the normal force. When the contact is sticking, the frictional force can be anything satisfying this constraint. When the contact is sliding, $f_\mathrm{t} = \mu f_\mathrm{n}$ and the direction of the friction force opposes the direction of sliding.
- Given a set of frictional contacts acting on a body, the wrenches that can be transmitted through these contacts is the positive span of the wrenches that can be transmitted through the individual contacts. These wrenches form a homogeneous convex cone. If the body is planar, or if the body is spatial but the contact friction cones are approximated by polyhedral cones, the wrench cone is also polyhedral.
- A homogeneous convex cone of planar wrenches in $\mathbb{R}^3$ can be represented as a convex region of moment labels in the plane.
- A body is in force closure if the homogeneous convex cone of contact wrenches from the stationary contacts is the entire wrench space ($\mathbb{R}^3$ or $\mathbb{R}^6$). If the contacts are frictionless, force closure is equivalent to first-order form closure.

12.5 Notes and References

The kinematics of contact draw heavily from concepts in linear algebra (see, for example, the texts [179, 118]) and, more specifically, screw theory [6, 127, 18, 2, 113]. Graphical methods for analysis of planar constraints were introduced by Reuleaux [147], and Mason introduced graphical construction of contact labels for planar kinematics and moment labels for representation of homogeneous wrench cones [108, 109]. Polyhedral convex cones, and their application in representing feasible twist cones and contact wrench cones, are discussed in [109, 66, 44, 55]. The formalization of the friction law used in this chapter was given by Coulomb in 1781 [31]. Surprising consequences of Coulomb friction are problems of ambiguity and inconsistency [94, 109, 112] and that infinite friction does not necessarily prevent slipping at an active contact [102].

Form closure and force closure are discussed in detail in the Handbook of Robotics [142]. In particular, that reference uses the term "frictional form closure" to mean the same thing that "force closure" means in this chapter. According to [142], force closure additionally requires that the hand doing the grasping be sufficiently capable of controlling the internal "squeezing" forces. Similar distinctions are made in [11] and the reviews [13, 12]. In this chapter we do not consider the details of the robot hand and adopt a definition of force closure based solely on the geometry and friction of the contacts.

The numbers of contacts needed for planar and spatial form closure were established by Reuleaux [147] and Somoff [174], respectively. Other foundational results in form and force closure are developed in [79, 120, 105] and are reviewed in [12, 142]. An overview of grasp quality metrics is given in [142]. The result that two friction cones that can "see" each other's base are sufficient for planar force closure was first reported in [125], and the result reviewed in this chapter on three-finger force-closure grasps in 3D appeared in [89]. Salisbury applied Grübler's formula to calculate the mobility of a grasped object using kinematic models of contact [111].

Second-order models of contact constraints were introduced by Rimon and Burdick [149, 148, 150, 151] and used to show that curvature effects allow form closure by fewer contacts.

Jamming and wedging in robotic insertion were described in [172, 124, 192], and the notion of a dynamic grasp was first introduced in [110].

An important class of methods for simulating systems of rigid bodies in frictional contact, not covered in this chapter, are based on solving linear and nonlinear complementarity problems [178, 130, 185]. These complementarity formulations directly encode the fact that if a contact is breaking, then no force is applied; if a contact is sticking, then the force can be anywhere inside the

friction cone; and if a contact is sliding, the force is on the edge of the friction cone.

General references on contact modeling and manipulation include Handbook of Robotics chapters [66, 142] and the texts by Mason [109] and Murray et al. [122].

12.6 Exercises

Exercise 12.1 Prove that the impenetrability constraint (12.4) is equivalent to the constraint (12.7).

Exercise 12.2 Representing planar twists as centers of rotation.

(a) Consider the two planar twists $\mathcal{V}_1 = (\omega_{z1}, v_{x1}, v_{y1}) = (1, 2, 0)$ and $\mathcal{V}_2 = (\omega_{z2}, v_{x2}, v_{y2}) = (1, 0, -1)$. Draw the corresponding CoRs in a planar coordinate frame, and illustrate $\text{pos}(\{\mathcal{V}_1, \mathcal{V}_2\})$ as CoRs.

(b) Draw the positive span of $\mathcal{V}_1 = (\omega_{z1}, v_{x1}, v_{y1}) = (1, 2, 0)$ and $\mathcal{V}_2 = (\omega_{z2}, v_{x2}, v_{y2}) = (-1, 0, -1)$ as CoRs.

Exercise 12.3 A rigid body is contacted at $p = (1, 2, 3)$ with a contact normal into the body $\hat{n} = (0, 1, 0)$. Write the constraint on the body's twist $\mathcal{V}$ due to this contact.

Exercise 12.4 A space frame {s} is defined at a contact between a stationary constraint and a body. The contact normal, into the body, is along the $\hat{z}$-axis of the {s} frame.

(a) Write down the constraint on the body's twist $\mathcal{V}$ if the contact is a frictionless point contact.

(b) Write down the constraints on $\mathcal{V}$ if the contact is a point contact with friction.

(c) Write down the constraints on $\mathcal{V}$ if the contact is a soft contact.

Exercise 12.5 Figure 12.29 shows five stationary "fingers" contacting an object. The object is in first-order form closure and therefore force closure. If we take away one finger, the object may still be in form closure. For which subsets of four fingers is the object still in form closure? Prove your answers using graphical methods.

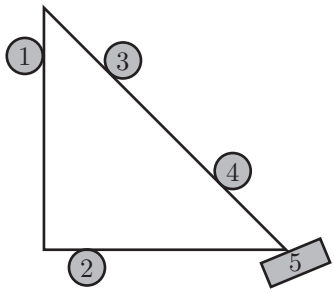

Figure 12.29: A triangle in contact with five stationary fingers, yielding first-order form closure and therefore force closure. Analyze the contact when one or more fingers are removed. The hypotenuse of the triangle is 45° from the vertical on the page, and contact normal 5 is 22.5° from the vertical.

Exercise 12.6 Draw the set of feasible twists as CoRs when the triangle of Figure 12.29 is contacted only by finger 1. Label the feasible CoRs with their contact labels.

Exercise 12.7 Draw the set of feasible twists as CoRs when the triangle of Figure 12.29 is contacted only by fingers 1 and 2. Label the feasible CoRs with their contact labels.

Exercise 12.8 Draw the set of feasible twists as CoRs when the triangle of Figure 12.29 is contacted only by fingers 2 and 3. Label the feasible CoRs with their contact labels.

Exercise 12.9 Draw the set of feasible twists as CoRs when the triangle of Figure 12.29 is contacted only by fingers 1 and 5. Label the feasible CoRs with their contact labels.

Exercise 12.10 Draw the set of feasible twists as CoRs when the triangle of Figure 12.29 is contacted only by fingers 1, 2, and 3.

Exercise 12.11 Draw the set of feasible twists as CoRs when the triangle of

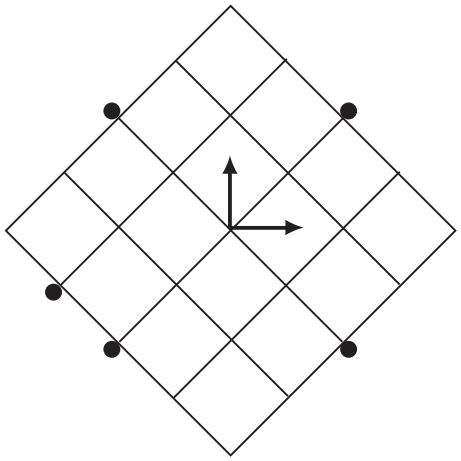

Figure 12.30: A 4×4 planar square restrained by five frictionless point contacts.

Figure 12.29 is contacted only by fingers 1, 2, and 4.

Exercise 12.12 Draw the set of feasible twists as CoRs when the triangle of Figure 12.29 is contacted only by fingers 1, 3, and 5.

Exercise 12.13 Refer again to the triangle of Figure 12.29.

(a) Draw the wrench cone from contact 5, assuming a friction angle $\alpha = 22.5^\circ$ (a friction coefficient $\mu = 0.41$), using moment labeling.

(b) Add contact 2 to the moment-labeling drawing. The friction coefficient at contact 2 is $\mu = 1$.

Exercise 12.14 Refer again to the triangle of Figure 12.29. Draw the moment-labeling region corresponding to contact 1 with $\mu = 1$ and contact 4 with $\mu = 0$.

Exercise 12.15 The planar grasp of Figure 12.30 consists of five frictionless point contacts. The square's size is 4×4.

(a) Show that this grasp does not yield force closure.

(b) The grasp of part (a) can be modified to yield force closure by adding one frictionless point contact. Draw all the possible locations for this contact.

Exercise 12.16 Assume the contacts shown in Figure 12.31 are frictionless point contacts. Determine whether the grasp yields force closure. If it does not,

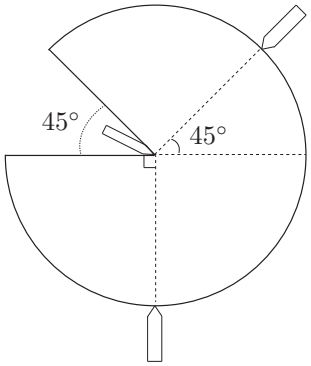

Figure 12.31: A planar disk restrained by three frictionless point contacts.

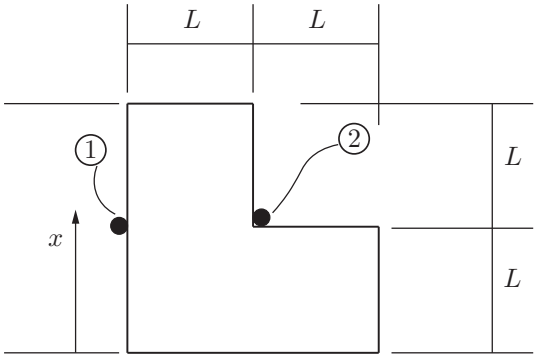

Figure 12.32: An L-shaped planar object restrained by two point contacts with friction.

how many additional frictionless point contacts are needed to construct a force closure grasp?

Exercise 12.17 Consider the L-shaped planar object of Figure 12.32.

(a) Suppose that both contacts are point contacts with friction coefficient $\mu = 1$. Determine whether this grasp yields force closure.

(b) Now suppose that point contact 1 has friction coefficient $\mu = 1$, while point contact 2 is frictionless. Determine whether this grasp yields force closure.

(c) The vertical position of contact 1 is allowed to vary; denote its height by x. Find all positions x such that the grasp is force closure with $\mu = 1$ for

contact 1 and $\mu = 0$ for contact 2.

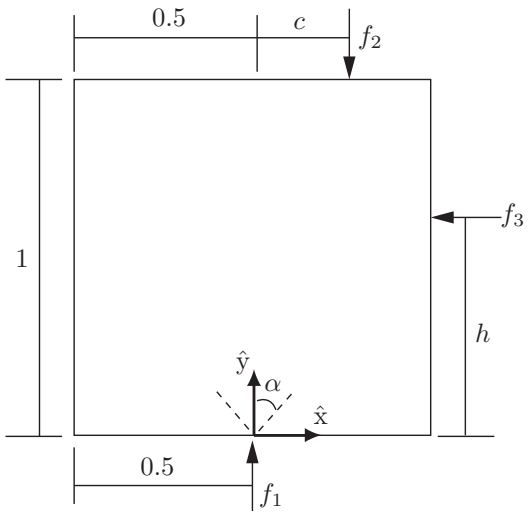

Figure 12.33: A square restrained by three point contacts.

Exercise 12.18 A square is restrained by three point contacts as shown in Figure 12.33: f_1 is a point contact with friction coefficient μ, while f_2 and f_3 are frictionless point contacts. If $c = \frac{1}{4}$ and $h = \frac{1}{2}$, find the range of values of μ such that grasp yields force closure.

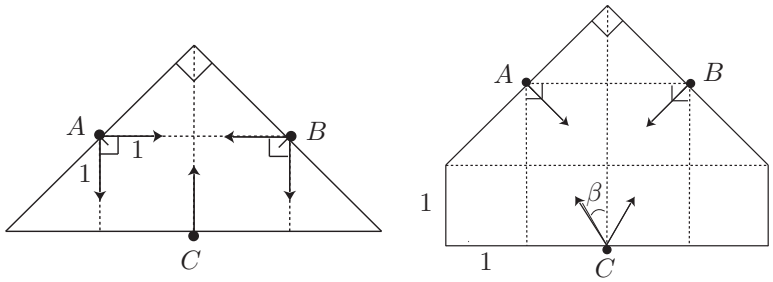

(a) Grasp for Exercise 12.19(a). (b) Grasp for Exercise 12.19(b).

Figure 12.34: Planar grasps.

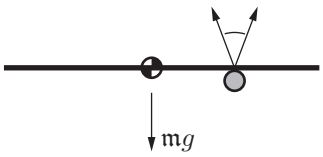

Figure 12.35: A zero-thickness rod supported by a single contact.

Exercise 12.19

(a) For the planar grasp of Figure 12.34(a), assume contact C is frictionless, while the friction coefficient at contacts A and B is $\mu = 1$. Determine whether this grasp is force closure.

(b) For the planar grasp of Figure 12.34(b), assume contacts A and B are frictionless, while contact C has a friction cone of half-angle β. Find the range of values of β that makes this grasp force closure.

Exercise 12.20 Find a formula for the minimum friction coefficient, as a function of n, needed for a two-fingered planar force-closure grasp of an n-sided regular polygon, where n is odd. Assume that the fingers can make contact only with the edges, not the vertices. If the fingers could also contact the vertices, how does your answer change? You can assume that the fingers are circular.

Exercise 12.21 Consider a table at rest, supported by four legs in frictional contact with the floor. The normal forces provided by each leg are not unique; there is an infinite set of solutions to the normal forces yielding a force balance with gravity. What is the dimension of the space of normal-force solutions? (Since there are four legs, the space of normal forces is four dimensional, and the space of solutions must be a subspace of this four-dimensional space.) What is the dimension of the space of contact-force solutions if we include tangential frictional forces?

Exercise 12.22 A thin rod in gravity is supported from below by a single stationary contact with friction, shown in Figure 12.35. One more frictionless contact can be placed anywhere else on the top or the bottom of the rod. Indicate all the places where this contact can be put so that the gravitational force is balanced. Use moment labeling to justify your answer. Prove the same using algebraic force balance, and comment on how the magnitude of the normal

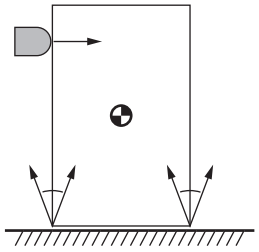

Figure 12.36: A frictionless finger pushes a box to the right. Gravity acts downward. Does the box slide flat against the table, does it tip over the lower right corner, or does it slide and tip over that corner?

forces depends on the location of the second contact.

Exercise 12.23 A frictionless finger begins pushing a box over a table (Figure 12.36). There is friction between the box and the table, as indicated in the figure. There are three possible contact modes between the box and the table: either the box slides to the right flat against the table, or it tips over at the right lower corner, or it tips over that corner while the corner also slides to the right. Which actually occurs? Assume a quasistatic force balance and answer the following questions.

(a) For each of the three contact modes, draw the moment-labeling regions corresponding to the table's friction cone edges active in that contact mode.
(b) For each moment-labeling drawing, determine whether the pushing force plus the gravitational force can be quasistatically balanced by the support forces. From this, determine which contact mode actually occurs.
(c) Graphically show a different support-friction cone for which the contact mode is different from your solution above.

Exercise 12.24 In Figure 12.37 body 1, of mass $\mathfrak{m}_1$ with center of mass at (x_1, y_1), leans on body 2, of mass $\mathfrak{m}_2$ with center of mass at (x_2, y_2). Both are supported by a horizontal plane, and gravity acts downward. The friction coefficient at all four contacts (at $(0,0)$, at (x_L, y), at $(x_L, 0)$, and at $(x_R, 0)$) is $\mu > 0$. We want to know whether it is possible for the assembly to stay standing by some choice of contact forces within the friction cones. Write down the six equations of force balance for the two bodies in terms of the gravitational forces and the contact forces, and express the conditions that must be satisfied for this

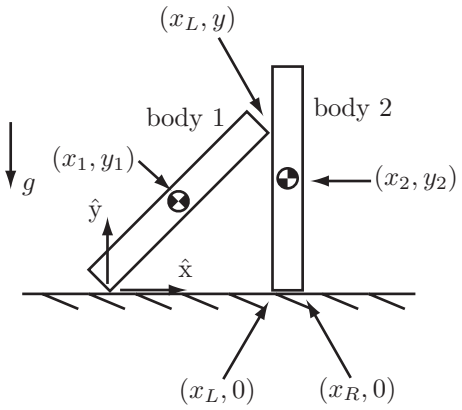

Figure 12.37: One body leaning on another (Exercise 12.24).

assembly to stay standing. How many equations and unknowns are there?

Exercise 12.25 Write a program that accepts a set of contacts acting on a planar body and determines whether the body is in first-order form closure.

Exercise 12.26 Write a program that accepts a set of contacts acting on a spatial body and determines whether the body is in first-order form closure.

Exercise 12.27 Write a program that accepts a friction coefficient and a set of contacts acting on a planar body and determines whether the body is in force closure.

Exercise 12.28 Write a program that accepts a friction coefficient and a set of contacts acting on a spatial body and determines whether the body is in force closure. Use a polyhedral approximation to the friction cone at each contact point that underestimates the friction cone and that has four facets.

Exercise 12.29 Write a program to simulate the quasistatic meter-stick trick of Example 12.10. The program takes as input: the initial x-position of the left finger, the right finger, and the stick's center of mass; the constant speed $\dot{x}$ of the right finger (toward the left finger); and the static and kinetic friction coefficients, where $\mu_s \geq \mu_k$. The program should continue the simulation until

the two fingers touch or until the stick falls. It should plot the position of the left finger (which is constant), the right finger, and the center of mass as a function of time. Include an example where $\mu_s = \mu_k$, an example where μ_s is only slightly larger than μ_k, and an example where μ_s is much larger than μ_k.

Exercise 12.30 Write a program that determines whether a given assembly of planar bodies can remain standing in gravity. Gravity g acts in the $-\hat{y}$-direction. The assembly is described by m bodies, n contacts, and the friction coefficient μ, all entered by the user. Each of the m bodies is described by its mass $\mathfrak{m}_i$ and the (x_i, y_i) location of its center of mass. Each contact is described by the index i of each of the two bodies involved in the contact and the unit normal direction (defined as into the first body). If the contact has only one body involved, the second body is assumed to be stationary (e.g., ground). The program should look for a set of coefficients $k_j \geq 0$ multiplying the friction-cone edges at the contacts (if there are n contacts then there are $2n$ friction-cone edges and coefficients) such that each of the m bodies is in force balance, considering gravity. Except in degenerate cases, if there are more force-balance equations ($3m$) than unknowns ($2n$) then there is no solution. In the usual case, where $2n > 3m$, there is a family of solutions, meaning that the force at each contact cannot be known with certainty.

One approach is to have your program generate an appropriate linear program and use the programming language's built-in linear-programming solver.

Exercise 12.31 This is a generalization of the previous exercise. Now, instead of simply deciding whether the assembly stays standing for a stationary base, the base moves according to a trajectory specified by the user, and the program determines whether the assembly can stay together during the trajectory (i.e., whether sticking contact at all contacts allows each body to follow the specified trajectory). The three-dimensional trajectory of the base can be specified as a polynomial in $(x(t), y(t), \theta(t))$, for a base reference frame defined at a particular position. For this problem, you also need to specify the scalar moment of inertia about the center of mass for each body in the assembly. You may find it convenient to express the motion and forces (gravitational, contact, inertial) in the frame of each body and solve for the dynamics in the body frames. Your program should check for stability (all contact normal forces are nonnegative while satisfying the dynamics) at finely spaced discrete points along the trajectory. It should return a binary result: the assembly can be maintained at all points along the trajectory, or not.